Stem Cell Reports
Review
OPEN ACCESS

Mouse Genetic Analysis of Bone Marrow Stem Cell Niches: Technological Pitfalls, Challenges, and Translational Considerations

Kevin G. Chen,[1,*] Kory R. Johnson,[2] and Pamela G. Robey[3,*]
[1]NIH Stem Cell Unit
[2]Information Technology and Bioinformatics Program
National Institute of Neurological Disorders and Stroke, National Institutes of Health, Bethesda, MD 20892, USA
[3]Skeletal Biology Section, National Institute of Dental and Craniofacial Research, National Institutes of Health, Bethesda, MD 20892, USA
*Correspondence: cheng@mail.nih.gov (K.G.C.), probey@dir.nidcr.nih.gov (P.G.R.)
https://doi.org/10.1016/j.stemcr.2017.09.014

The development of mouse genetic tools has made a significant contribution to the understanding of skeletal and hematopoietic stem cell niches in bone marrow (BM). However, many experimental designs (e.g., selections of marker genes, target vector constructions, and choices of reporter murine strains) have unavoidable technological limitations and bias, which lead to experimental discrepancies, data reproducibility issues, and frequent data misinterpretation. Consequently, there are a number of conflicting views relating to fundamental biological questions, including origins and locations of skeletal and hematopoietic stem cells in the BM. In this report, we systematically unravel complicated data interpretations *via* comprehensive analyses of technological benefits, pitfalls, and challenges in frequently used mouse models and discuss their translational relevance to human stem cell biology. Particularly, we emphasize the important roles of using large human genomic data-informatics in facilitating genetic analyses of mouse models and resolving existing controversies in mouse and human BM stem cell biology.

Introduction

Genetically modified mouse models have been extensively used to trace stem cell niches, evaluate stem cell identities, and provide translational insights into human stem cell biology. Currently, we still face considerable experimental discrepancies and data reproducibility issues related to the use of mouse genetic models, which have led to several major controversies in fundamental biological questions in the bone marrow (BM) stem cell field. For example, the precise locations of hematopoietic stem cell (HSC) niches, which are predominantly determined by the use of various mouse reporter genes, are currently under debate (Acar et al., 2015; Asada et al., 2017; Kunisaki et al., 2013; Oguro et al., 2013). Moreover, "mesenchymal stem cells" are a vague and confusing concept, which was primarily based on "bone marrow stromal cells" (Friedenstein et al., 1966; Owen and Friedenstein, 1988) and on multipotent skeletal stem cells (SSCs), without the use of definitive markers (Bianco and Robey, 2015). Furthermore, it is unclear whether local neural crest cells could directly contribute to SSCs in BM (Isern et al., 2014; Morikawa et al., 2009; Zhou et al., 2014). Thus, BM stem cells represent a more diffuse-and-complex biological area, having many unidentified variables that are responsible for existing experimental discrepancies and data irreproducibility (Morrison, 2014). Nonetheless, it appears that all the above controversies are, at least, associated with one common methodological basis; i.e., the differential use of mouse reporter strains.

During the past two decades, marker gene identifications combined with cell lineage tracing using reporter mouse strains have had a major impact on understanding the complexity of cellular dynamics and commitments of murine BM stem cell niches at various developmental stages. However, choices of marker genes, constructions of reporter murine strains, and even experimental designs have unavoidable bias, which have limited our understanding of BM stem cell biology (reviewed in Bianco and Robey, 2015; Kfoury and Scadden, 2015; Mendez-Ferrer et al., 2015; Morrison and Scadden, 2014). Current technologies used to identify BM stem cells mainly rely on various mouse reporter strains based on limited numbers of marker genes (e.g., nestin [*Nes*], leptin receptor [*Lepr*], *Cspg4*/*NG2*, and *Wnt-1*). Perplexingly, these marker genes usually have high levels of expression in non-BM tissues or organs, thus having limited specificity in BM. For instance, in mouse embryos, *Nes*, *Lepr*, *Cspg4*, and *Wnt-1* all have higher levels of expression in the brain than in the BM. At present, many unmanageable variables in mouse experiments stem from genetically engineered reporter genes in mouse strains. Therefore, optimizing murine models to resolve existing controversies and to translate the information from animal models into human BM biology has been challenging.

To accurately define diverse BM cell lineages and differentiation, in this review, we systematically untangle the complicated data interpretation using various mouse genetic models. We aim to do the following: (1) briefly discuss the advantages of mouse genetic models and try to resolve inconsistencies, (2) shed light on the technological advantages, pitfalls, and challenges in the development of BM stem cell lineages, and (3) examine the translational relevance of murine models, and utilize existing large human genomic datasets to facilitate data interpretation. Technically, we present this review as a dedicated resource, in which our detailed analyses of the *pros* and *cons*

of different mouse strains (in the main text and in Tables 1 and S1) would enable scientists to efficiently grasp principles of designing mouse genetic models and of choosing appropriate mouse strains of interest. The genomic and molecular analyses, available in Figures 1, 2, 3, 4, and 5, would help researchers to prospectively understand the translational process based on existing genomic databases. Hence, this resource review may be suitable for a broad range of investigators, scientists, biologists, and trainees in different stem cell fields, particularly for scientists working on the hematological and skeletal systems.

Mouse Genetic Models: Advantages and Problems Solved

Mouse genetic models have dramatically advanced our understanding of many fundamental developmental processes in both the skeletal and hematological systems, thereby accelerating the processes of translational medicine (Bianco et al., 2013; Frenette et al., 2013; Morrison and Scadden, 2014). These mouse models offer cell lineage mapping *in vivo*, a powerful approach to study specific cell types, numbers, physiological and pathological states, and particularly cell signaling pathways in stem cell niches (Tables 1 and S1).

Stem cell niches can be briefly defined as a specific microenvironment that contains and sustains stem cells in an undifferentiated state. The basic components of a BM stem cell niche comprise BM stroma, extracellular matrices, HSCs, SCCs, Cxcl12-abundant reticular (CAR) cells, adipocytes, endothelial cells, and different types of stromal cells not fully defined to date. These niche-supporting cells secrete specific niche factors encoded by many HSC niche maintenance genes (such as *Cxcl12*, *KitL*, *Angpt1*, and *Lepr*) at restricted regions and mediate many intercellular interactions (Isern et al., 2014). Several known niche-supporting cells include CAR cells (Sugiyama et al., 2006), *NG2*$^{+}$/*Nes*-GFP^{high} cells (Kunisaki et al., 2013), and *Lepr*-Cre^{+}/*Nes*-GFP^{low} cells (Zhou et al., 2014). Technically, niche-associated gene promoter or enhancer activity as well as mRNA expression can be monitored and targeted by different fluorescent reporter proteins such as GFP. Thus far, mouse genetic models combined with imaging analysis have been the most widely used tool to successfully answer long-standing questions in developmental biology, which include the origins, identities, and locations of postnatal SSCs and HSCs. It is clear now that the major source of SCCs in human BM is tightly associated with CD146^{+}/CD45^{-}/Ter119^{-} reticular pericytes (Sacchetti et al., 2016) and *Lepr*-Cre^{+}/*Nes*-GFP^{low} cells near perisinusoids (Zhou et al., 2014) in mice. The major HSC niche has also been confidently localized at BM perivascular regions containing specific types of stromal cells (Acar et al., 2015; Kunisaki et al., 2013).

Tables 1 and S1 summarize a significant amount of data, with point-to-point interpretations and comments of each reporter mouse strain, related to BM cell lineage development, perivascular stromal cells, and neural crest cells. However, to better understand the *pros* and *cons* of genetically modified strains, we comprehensively analyzed two frequently used transgenes (i.e., *Nes* and *Lepr*) at different developmental stages (Table S1; Figure 1). These two individual genes are chosen, not only for their frequent use in BM niche studies, but also for their transcriptional activities that have empowered us to mark several important niche-supportive cell populations (i.e., *Nes*-GFP^{high}, *Nes*-GFP^{low}, and *Lepr*-Cre^{+} BM stromal cells) (Kunisaki et al., 2013; Zhou et al., 2014). Accordingly, there is an increasing body of data generated from using these mouse models (Table S1). For example, combined with other transgene reporters such as *NG2*-CreER^{TM}, a tamoxifen-inducible Cre recombinase-estrogen fusion protein driven by the *NG2* promoter-enhancer, scientists were able to identify two important BM cell populations. These two distinct cell populations; i.e., *NG2*-CreER^{TM+}/*Nes*-GFP^{high} and *Lepr*-Cre^{+}/*Nes*-GFP^{low} cells, likely constitute a distinct HSC niche at the periarteriolar and a major SSC source at the perisinusoidal regions (Kunisaki et al., 2013; Zhou et al., 2014). The existence of distinct HSC niches, presumably with different functions, is currently an important topic under debate (Acar et al., 2015; Asada et al., 2017; Kunisaki et al., 2013; Oguro et al., 2013). Despite the enthusiasm of applying transgene-based models for *in vivo* cell-fate mapping, there are emerging controversial concepts, inconsistent data, and inappropriate data interpretation due to the limitations of mouse genetic systems.

Mouse Genetic Models: Disadvantages, Pitfalls, and Experimental Discrepancies

Noticeably, there are numerous limitations of mouse genetic models, which can be introduced by the experimental design of generating genetically engineered mice, to experimental data collection and interpretation. In general, the causes of experimental variability could be classified into the following four major categories, which include the following: (1) the designs of transgenes or targeting vectors used for generating transgenic mice; (2) random chromosomal integrations of genetically identical transgenes or similar transgenes; (3) methods of gene expression (e.g., constitutive versus inducible gene expression systems) and associated cellular cytotoxicity; and (4) complicated dynamic changes of cellular and molecular states of cells in BM throughout development. In the following sections, we will use some representative examples to highlight the above-mentioned major causes of experimental variability and discrepancies.

Table 1. Representative Analyses of Marker Genes Used for Bone Marrow and Skeletal Stem Cell Identities

Mouse Strains	Major Descriptions	Authors' Comments	References
Col2.3-GFP transgenic mice	express GFP in osteoblasts and osteocytes under the control of the 2.3-kb rat Col 1a1 (procollagen, type 1, alpha 1) promoter	useful for studying bone development and osteoblast lineage tracing; wary of rat subspecies sequence effects	Kalajzic et al., 2002
Cxcl12-dsRed	▶ express dsRedE2 from the mouse endogenous *Cxcl12* promoter ▶ the dsRed knockin produces a strong loss-of-function allele ▶ dsRed recognized by anti-RFP	useful for identifying Cxcl12-expressing perivascular stromal cells and endothelial cells in the bone marrow	Ding and Morrison, 2013
Cxcl12-GFP knockin mice	highly enriched in Cxcl12-abundant reticular (CAR) cells within the intratrabecular space in the bone marrow	endothelial cells and the endosteal surface osteoblasts show faint or undetectable GFP signals	Ara et al., 2003; Sugiyama et al., 2006
Gt(ROSA)26Sor$^{tm1(HBEGF)Awai}$	▶ have the simian diphtheria toxin receptor (*DTR*; from simian Hbegf) inserted into the Gt(ROSA)26S or the ROSA26 locus, whose expression is suppressed by an upstream loxP-flanked STOP sequence ▶ inducible expression of *DTR* by *Cre* recombinase	suitable for ablation of cells that express DTR following diphtheria toxin treatment	Buch et al., 2005
Lepr$^{fl/fl}$	B6.129P2-Lepr$^{tm1Rck/J}$, also known as: ObR^{Flox} ▶ have loxP sites on either side of exon 1 of the mouse *Lepr* gene ▶ delete exon 1 when bred to a Cre recombinase-expressing mice under a tissue-specific promoter	▶ useful in studies of obesity and *Lepr* related cell lineage analysis ▶ beware of expression of short *Lepr* isoforms that are initiated after exon 1	Cohen et al., 2001 http://www.jax.org/
Lepr-Cre	L B6.129-Lepr$^{tm2(Cre)Rck/J}$ (*Lepr*-Cre); the targeting vector contains an IRES-NLS-*Cre* and a *neo* (flanked by frt sites) inserted immediately 3′ of the stop codon in the last exon of the *Lepr* gene	transcripts may terminate in many *Lepr* transcript variants that do not contain the last exon of the canonical Lepr isoform (Lepr-B)	DeFalco et al., 2001
Mx-1-Cre, transgenic mice	B6.Cg-Tg(*Mx1*-cre)1Cgn/J, also known as *Mx*-Cre and *Mx1*-Cre (BALB/c): the *Mx-1*-Cre transgene contains Cre recombinase under the control of the *Mx-1* promoter that is silent in healthy mice	▶ the *Mx-1* promoter is highly sensitive to interferon α/β and synthetic double-stranded RNAs, e.g., poly(I:C) ▶ cautions should be taken when experimental conditions involving interferons and exogenous double-stranded RNAs	Kuhn et al., 1995 http://www.jax.org/
Nes-Cre	Cre recombinase is expressed under the control of the 5.8-kb rat *Nes* promoter and the 1.8-kb intron 2 enhancer element	▶ no ER^{T2} fragment in the construct ▶ genomic orientation of the *Nes* genomic elements is similar to that of *Nes*-GFP described by Mignone et al. (2004)	Tronche et al., 1999

(*Continued on next page*)

Table 1. *Continued*

Mouse Strains	Major Descriptions	Authors' Comments	References
Nes-CreER^{T2} transgenic mice	C57BL/6-Tg(Nes-cre/ER^{T2})KEisc/J: ▶ express the T2 mutant form of a Cre-estrogen receptor fusion (Cre-ER^{T2}) under the control of the 1.8-kb rat *Nes* intron-2 enhancer (i2E) element and a 160-bp HSV TK promoter followed by an SV40 polyA site ▶ Cre-ER^{T2} fusion protein activity: inducible to the nucleus at high levels following binding of tamoxifen, which deletes the floxed sequences in cells of bred mice ▶ the *Nes*-CreER^{T2} transgene directs *Cre* expression in *Nes*-expressing cells in the subventricular zone (SVZ) and subgranular zone (SGZ) ▶ useful for studying the lineage commitments in both adult and developing mouse brains	▶ the 4.2-kb transgene fragment excluded the majority of the rat 5′ promoter sequence ▶ the intron-2 enhancer element orientated differently from that of the *Nes*-GFP construct (Mignone et al., 2004); thus may have differential transcriptional effects ▶ a complicated inducible system, involving mixed estrogen-agonist effects of tamoxifen on the impairment of bone growth, apoptosis in growth plate chondrocytes in cultured rat metatarsal bones, and signal transductions between endothelial cells and pericytes	Balordi and Fishell, 2007; Chagin et al., 2007; Feil et al., 1997; Karimian et al., 2008; Lagace et al., 2007; Zimmerman et al., 1994
Nes-GFP	Tg(Nes-EGFP)33Enik: a *Nes*-GFP reporter in transgenic mice, driven by the 5.8 promoter and 1.8-kb intron 2 enhancer of the rat *Nes* gene	▶ predicting CNS neural stem cell or progenitor specific promoter and intron 2 enhancer transcriptional activity ▶ rat sequence in a mouse model ▶ expected differences among *Nes*-GFP, *Nes*-Cre, and *Nes*-CreER^{T2} strains	Lendahl et al., 1990; Mignone et al., 2004; Zimmerman et al., 1994
NG2-CreER^{TM}	B6.Cg-Tg(Cspg4-Cre/Esr1*)BAkik/J, ▶ *NG2*-CreER^{TM} BAC transgenic mice ▶ tamoxifen-inducible Cre (CreER^{TM}) under the control of the mouse *NG2* (*Cspg4*) promoter/enhancer	useful for inducible Cre recombinase expression in NG2-expressing glia and other cell types	Zhu et al., 2011; http://www.jax.org/
P0-Cre	transgenic mice expressing Cre recombinase directed by the myelin protein zero (*P0*) gene promoter	genetic tools for labeling neural crest cell lineages such as Schwann cells	Feltri et al., 1999; Yamauchi et al., 1999
Prx1-Cre	B6.Cg-Tg(Prrx1-cre)1Cjt/J: expresses *Cre* under the control of a *Prrx1*-derived enhancer	useful for studying limb bud development and patterning	Logan et al., 2002
Wnt1-Cre	▶ carrying Cre cDNA between *Wnt1* promoter and enhancer ▶ widely used in the study of brain development, the neural crest and its derivatives	▶ phenotypes can be complicated by ectopic activation of canonical Wnt/β-catenin signaling related to increased Wnt1 protein expression ▶ may be used as a gain-of-function model for studying Wnt signaling mechanisms in middle brain development	Danielian et al., 1998; Lewis et al., 2013

(*Continued on next page*)

Table 1. ***Continued***

Mouse Strains	Major Descriptions	Authors' Comments	References
Wnt1-Cre2	Cre expression under the control by 1.3-kb 5′ promoter and 5.5-kb 3′ enhancer	▶ serve similar purposes to the original *Wnt1*-Cre (Danielian et al., 1998) ▶ deprived of complicated phenotypes associated with gain of function of Wnt1	Lewis et al., 2013

Cre, Cre recombinase; Cxcl12, chemokine (C-X-C motif) ligand 12; GFP, green fluorescent protein; HSV, herpes simplex virus; IRES, internal ribosome entry site; Neo, neomycin resistance gene; NLS, nuclear localization signal; RFP, red fluorescent protein; TK, thymidine kinase.

Mouse Genetic Model Designs: Genomic Elements, Orientations, and Gene Reporter Data Interpretation

It is worth noting that the choice of promoter sequences and enhancer elements in a reporter construct might have a major impact on reporter activity in mouse models. As far as *Nes*-GFP and *Nes*-CreER^{T2} mouse models are concerned, both transgenes certainly report transcriptional activation of the *Nes* gene. However, their transcriptional activities are apparently controlled by two different genetic systems (Figure 2A). *Nes*-GFP expression is driven essentially by the 5′ 5.8-kb promoter and the 1.8-kb intron 2 enhancer (i2E) (Table S1; Figure 2A). However, in *Nes*-CreER^{T2} transgenic mice, a tamoxifen-inducible Cre-estrogen fusion cassette (i.e., CreER^{T2}) is driven by a thymidine kinase promoter under the control of the 5′ i2E element (Figure 2A). Thus, the 4.2-kb transgene fragment excludes the majority of the rat 5′ *Nes* promoter sequence, which has a different genomic orientation from that of the *Nes*-GFP construct (Mignone et al., 2004).

Not surprisingly, some experimental discrepancies have been observed from these two genetically different transgenes. *Nes*-CreER^{T2+} and *Nes*-GFP^{+} cells were not co-localized, but differentially presented at the prenatal stage in BM (Table S1). *Nes*-CreER^{T2+} cells are likely involved in fetal bone development based on their locations near the osteochondral junction and trabecular bone at the prenatal stage, but not in committing to neonatal and postnatal bone development (Isern et al., 2014). It appears that *Nes*-CreER^{T2+} cells co-localize with *Nes*-GFP^{+} pericytes at the neonatal stage (i.e., P0 to P14) (Isern et al., 2014). Seemingly, *Nes*-GFP^{+} stromal cells did not contribute to fetal endochondrogenesis (Isern et al., 2014), but subsequently initiated their role in specifying osteoblasts at the neonatal stage (i.e., P0 to P10) (Ono et al., 2014). Consistently, a *Lepr*-Cre^{+}/*Nes*-GFP$^{low/+}$ cell population, without *Nes*-CreER^{T2} expression, was shown to be a major SSC source in the mouse BM at a postnatal stage (Zhou et al., 2014). Thus, *Nes*-CreER^{T2+} and *Nes*-GFP^{+} cells have distinct functions in specifying SSC lineage development in BM. Still, the underlying molecular basis for the above discrepancies between *Nes*-GFP and *Nes*-CreER^{T2} mouse strains remains to be elucidated (Isern et al., 2014; Ono et al., 2014).

We speculate that the above discrepancies could be partially explained by the different orientation of their genomic and vector elements (Figure 2A). The *Nes*-CreER^{T2} transgene, containing the i2E, likely functions as a weaker reporter of neuronal enhancer complexes (due to its orientation). *Nes*-GFP, containing the *Nes* promoter and i2E and mimicking the orientation of the endogenous *Nes* gene, reports a wide-range of transcriptional activities, ranging from weak to strong GFP signals, at different developmental stages (Figure 2A). Likewise, there are two transcriptional activities that regulate *Nes*-GFP, which are differentially associated with specification of the SSC lineage (defined by *Lepr*-Cre^{+}/*Nes*-GFP$^{low/+}$) and with the periarteriolar HSC niche (defined by *NG2-CreER^{TM+}*/*Nes*-GFP^{high} cells).

In the case of *Lepr* regulation, one potential misinterpretation of transcriptomic data might also be due to the orientation of reporter genes (e.g., GFP) that are used to depict transcriptional activity of different transcript variants. The *Lepr* has a large and complicated genomic organization, which transcribes multiple mRNA variants from a promoter (designated as P2), which is different from that of humans (P1) (Figure 1B). Interestingly, the mouse P2 promoter-initiated transcripts are often terminated at different exons that are proximal to mouse exon 19 (exon 20 in the human counterpart) of the canonical *Lepr gene* (Figure 1B). Therefore, a knockin reporter immediately after exon 19 in mice only depicts the canonical *Lepr* transcriptional activities (DeFalco et al., 2001), likely masking or underscoring the contribution of different *Lepr* isoforms or alternative transcripts (terminated at a different exon) to lineage differentiation (Kunisaki et al., 2013; Zhou et al., 2014). In general, *Nes*- or *Lepr*-driven transgene or knockin gene expression seems far more complicated than their endogenous mRNA and protein expression at different developmental stages (Table S1). Therefore, genomic elements and their orientations must be taken into consideration when designing or choosing desired genetic models, and interpretation of transgene reporter data.

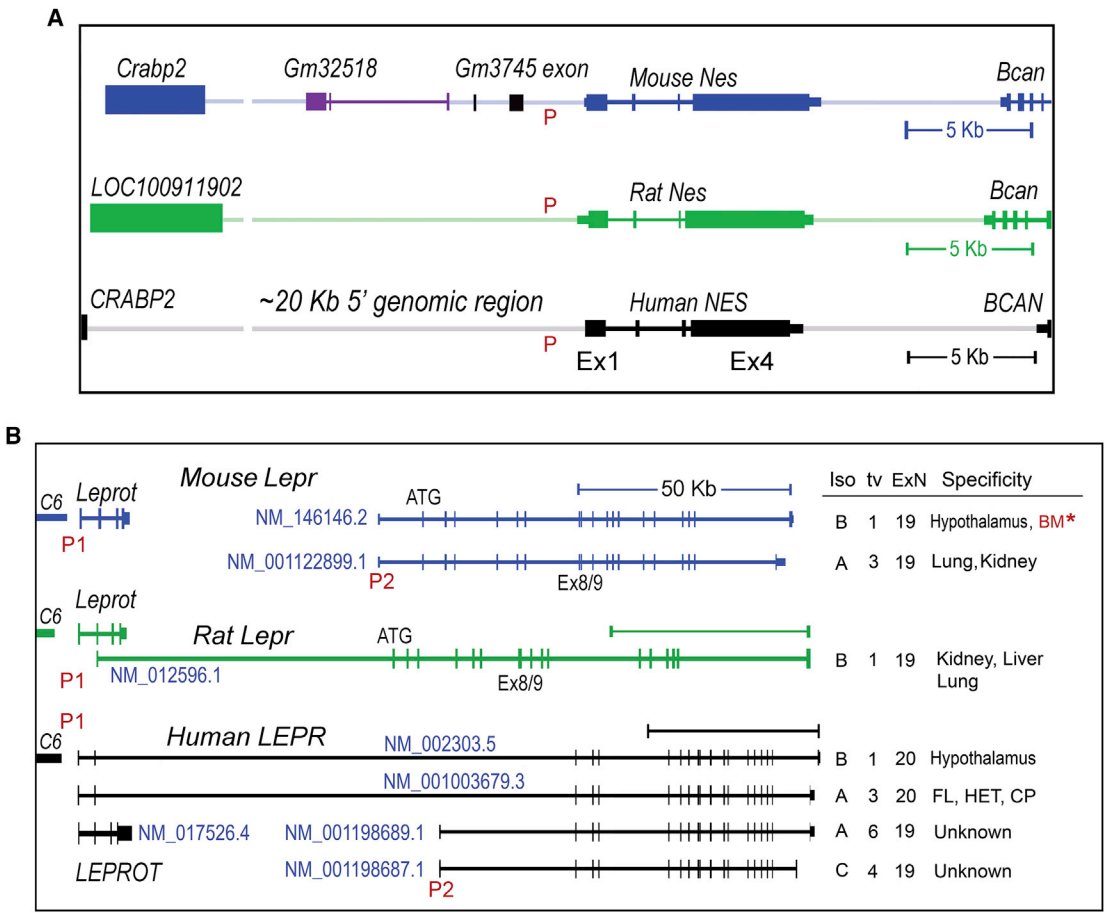

Figure 1. Genomic Organization of the Nestin and Leptin Receptor Genes

(A) Nestin and (B) leptin receptor genes in mice, rats, and humans. The graphs were created based on recent data from both the National Center for Biotechnology Information (NCBI) (www.ncbi.nlm.nih.gov) and the UCSC Genome Browser (genome.ucsc.edu). The accession numbers for leptin receptor isoforms are: NM_146146.2 (mouse *Lepr-B* isoform, transcript variant 1, 19 exons), NM_001122899.1 (mouse *Lepr-A*, transcript variant 3, 19 exons), NM_012596.1 (rat *Lepr-B*, 19 exons), and NM_002303.5 (human *LEPR-B*, transcript variant 1, 20 exons), NM_001003679.3 (human *LEPR-A*, transcript variant 3, 20 exons), NM_001198689.1 (human *LEPR-A*, transcript variant 6, 19 exons), and NM_001198687.1 (human *LEPR-C*, transcript variant 4, 19 exons). Representative leptin receptor isoforms, transcript variant identification numbers, exon numbers, and tissue-specific expression patterns were briefly indicated in the right panel. Of note, the asterisk sign (*) indicates that mouse bone marrow (BM) stromal cells express the *Lepr isoform b* based on the existence of *Lepr*-Cre^{+} cells around sinusoids of the BM (Zhou et al., 2014) and the NLS-Cre cassette (in the *Lepr*-Cre transgene), which is inserted into the 3′ of the stop codon at exon 19 of the transcript variant 1 (DeFalco et al., 2001).

E or Ex, exon; ExN, exon numbers; FL, fetal liver; HET, hematopoietic tissues; I, intron; Iso, leptin receptor protein isoform; *Lepr/LEPR*, the leptin receptor gene; *Leprot/LEPROT*, leptin receptor overlapping transcript; *Nes/NES*, the gene coding for nestin; tv, transcript variant; P, promoter.

Random Chromosomal Integration of Transgenes

Besides the interference from genomic elements and their orientations, random chromosomal integrations of the same transgene could be another major factor that explains different transgene expression patterns in mouse BM. Theoretically, no two transgenic lines are created equal when the genomic elements are randomly integrated in the mouse genome. The variability of transgenic lines has created some confusion and misinterpretation of data when using transgenic reporter as markers. In the case of the *Nes* gene, there are approximately nine *Nes*-CreER^{T2} transgenic lines that have been designed and used to study mouse neural stem cells and progenitors (Sun et al., 2014). However, the expression patterns of these *Nes*-CreER^{T2} lines vary greatly in the mouse brain, apparently because of random chromosomal integration. Only very small subset lines expressed *Nes*-CreER at the neurogenic zones of the adult brain, like that of the endogenous *Nes* gene

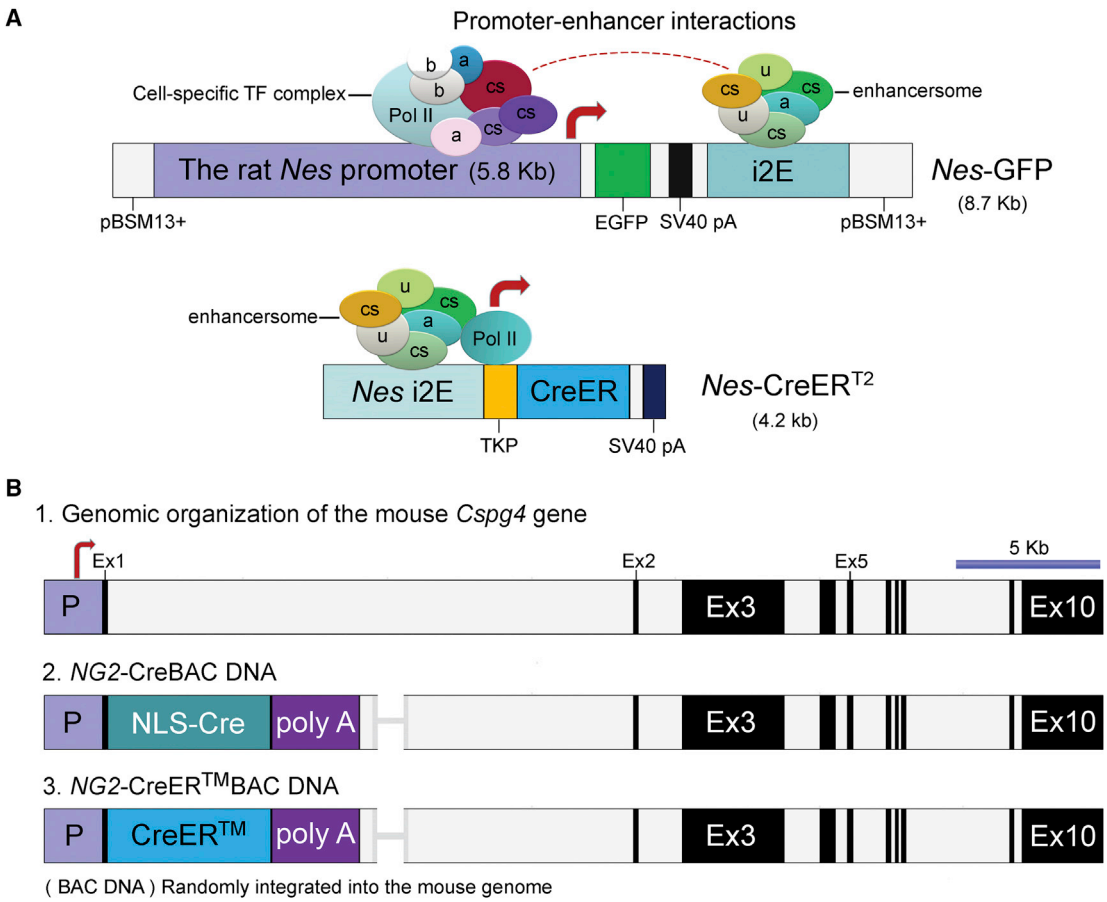

Figure 2. DNA Transgene Expression Vectors and Regulatory Mechanisms

(A) Transgene expression vectors based on the rat *Nes* gene. Top panel: *Nes*-GFP, subcloned into the pBSM13 vector, contains the 5.8-kb rat *Nes* promoter and the 1.8-kb neural-specific intron-2 enhancer fragment (i2E), which flanked the enhanced version of GFP (EGFP). The 8.7-kb final construct, mimicking the arrangement of the regulatory sequences of the *Nes* or *NES* found in the rat, mice, and humans, was used for the pronuclear injections of the fertilized oocytes (Mignone et al., 2004). Lower panel: *Nes*-CreER^{T2} comprises the T2 mutant form of a Cre recombinase-estrogen receptor fusion (Cre-ER^{T2}) (Feil et al., 1997) under the control of a thymidine kinase promoter (TKP) driven by the 1.8-kb i2E as described in the top panel (Balordi and Fishell, 2007). In *Nes*-GFP transgenic mice, a cell-specific transcriptional complex at the promoter might interact with the neural-specific intron-2 enhancersome, thereby mediating different gene expression patterns in miscellaneous cell types including BM cells. However, in the case of *Nes*-CreER^{T2} mice, the transgene is largely driven by the intron 2 enhancersome.

(B) Transgene expression vectors based on the chondroitin sulfate proteoglycan four gene (*Cspg4*), also known as *NG2* (neural/glial gene). (1) Genomic organization of the *Cspg4* gene is based on the recent genomic information from the NCBI sequence (NM_1390012) with a scale bar (5 kb). (2 and 3) *NG2*-CreBAC (Zhu et al., 2008) and *NG2*-CreER^{TM}BAC (Zhu et al., 2011) DNAs were used for generating *NG2*-Cre and *NG2*-CreER^{TM} transgenic mice, respectively. In brief, a 208-kb mouse bacterial artificial chromosome (BAC) containing the entire *Cspg4* gene was modified by introducing a Cre recombinase cDNA with a nuclear localization signal (NLS) or a CreER^{TM} cDNA (Danielian et al., 1993; Littlewood et al., 1995) into exon 1 of the *Cspg4* gene, followed by a rabbit β-globin polyadenylation sequence, poly(A). These two transgenes were microinjected into the pronucleus of fertilized oocytes from C57BL/6J mice to generate the transgenic lines of interest.

a, adaptor protein(s); b, basal transcriptional factor(s); Cre-ER^{T2}, Cre recombinase fused to the human estrogen receptor ligand-binding domain with a triple mutation (i.e., G400V/M543A/L544A), which does not bind its natural ligand (17β-estradiol); Cre-ER^{TM}, Cre recombinase fused to a G525R mutant form of the mouse estrogen receptor ligand-binding domain; cs, cell-specific, Ex, exon; i2E, the intron 2 enhancer fragment of the rat *Nes* gene; P, promoter; Pol II, RNA polymerase II; SV40 pA, the polyadenylation sequences from the simian virus 40; TF, transcriptional factor; TKP, a 160-bp herpes simplex virus (HSV) thymidine kinase (TK) promoter; u, unidentified factor(s).

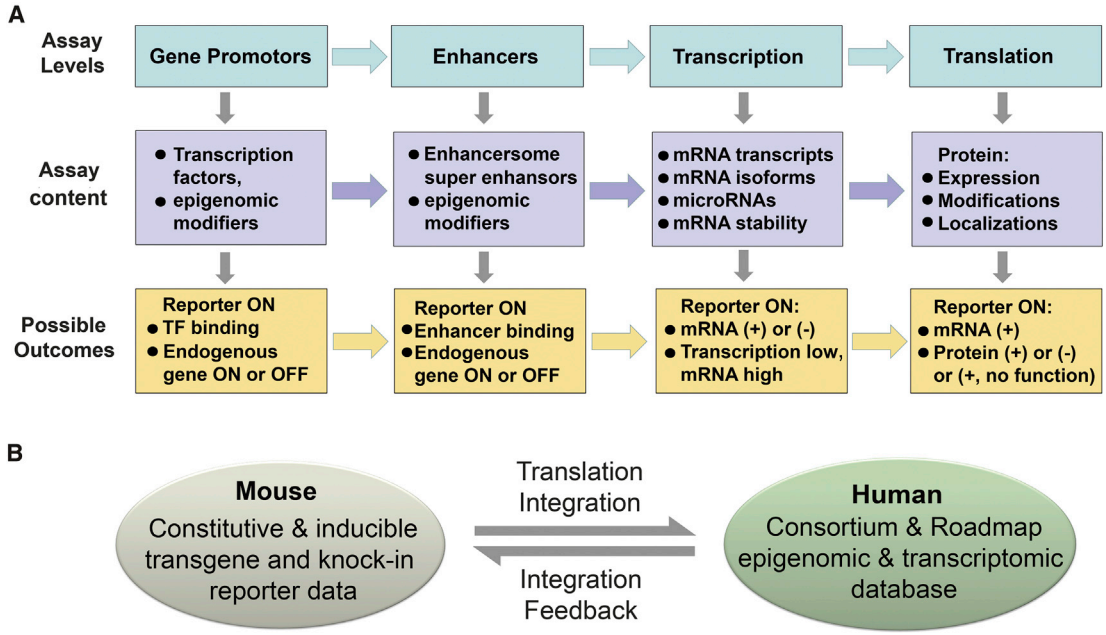

Figure 3. Gene Regulation, Data Interpretation, and Integration

(A) Regulation of transgene at different molecular levels. Transgene reporter expression may or may not overlap with endogenous gene expression patterns. With regard to a transgene reporter activation, various experimental outcomes may be possible, which need to be confirmed by additional downstream assays (e.g., mRNA and protein expression).

(B) A scheme of data integration between mouse transgene reporter data and human epigenomic databases. Data from mouse genetic models may be directly translated and integrated into human BM biology given that they shared highly similar genomic structures and regulatory elements. Existing genomic and epigenomic databases can be also used to facilitate mouse data interpretation and help design humanized mouse models.

(Sun et al., 2014). Thus, each individual line should be fully characterized prior to use for a specific need.

Gene Expression Methods: Constitutive Versus Inducible Expression

It is conceivable that different gene manipulations would also have a significant impact on their expression patterns. As already discussed above, *Nes*-GFP and *Nes*-CreER^{T2} have different transgene expression patterns in the BM (Isern et al., 2014; Ono et al., 2014; Zhou et al., 2014), which may be partially explained by their differences in regulatory elements and their orientations in the expression vectors (Figure 2A). Moreover, these two transgenes also differ in the regulatory elements that control their expression. *Nes*-GFP has a constitutively active *Nes* promoter and i2E in neurogenic cells (Figure 2A). *Nes*-CreER^{T2} contains a tamoxifen-inducible CreER^{T2}. Nevertheless, the definite role of CreER^{T2} in the contribution to experimental discrepancies remains to be determined for the complexity of the two transgene systems. Moreover, it also remains to be established whether a constitutive versus inducible modification would lead to a significant experimental difference or discrepancy.

Fortunately, a pairwise comparison between another two transgene expression systems (i.e., *NG2*-Cre and *NG2*-CreER^{TM}), in which the genetic elements (i.e., the nuclear localization signal [NLS] and CreER^{TM}) that control constitutive and inducible expression, respectively, are the only difference (Figure 2B). This comparison presents a convincingly positive answer to the above question (Asada et al., 2017). *NG2*-Cre, with a constitutively active NLS, marks BM stromal cells at both periarteriolar and sinusoidal areas; whereas *NG2*-CreER^{TM}, with a tamoxifen-inducible Cre-ER^{TM}, preferentially marks periarteriolar cells, presumably presenting distinct HSC niche-supporting function (Asada et al., 2017). Thus, *NG2*-Cre- and *NG2*-creER^{TM}-marked cells showed differential HSC niche-supporting functions, in which *NG2*-Cre^{+}, but not *NG2*-creER^{TM+}, cells are the source of the major HSC niche factor, Scf, whose deletion in *NG2*-Cre mice led to a defect in multi-lineage reconstitution in the BM (Asada et al., 2017). Clearly, these results provide insights into how different genetic approaches can impact on experimental conclusions, thereby presenting, at least partial resolution, of the current debate between the existence of distinct and uniform HSC niches in BM (Acar et al., 2015; Kunisaki et al., 2013).

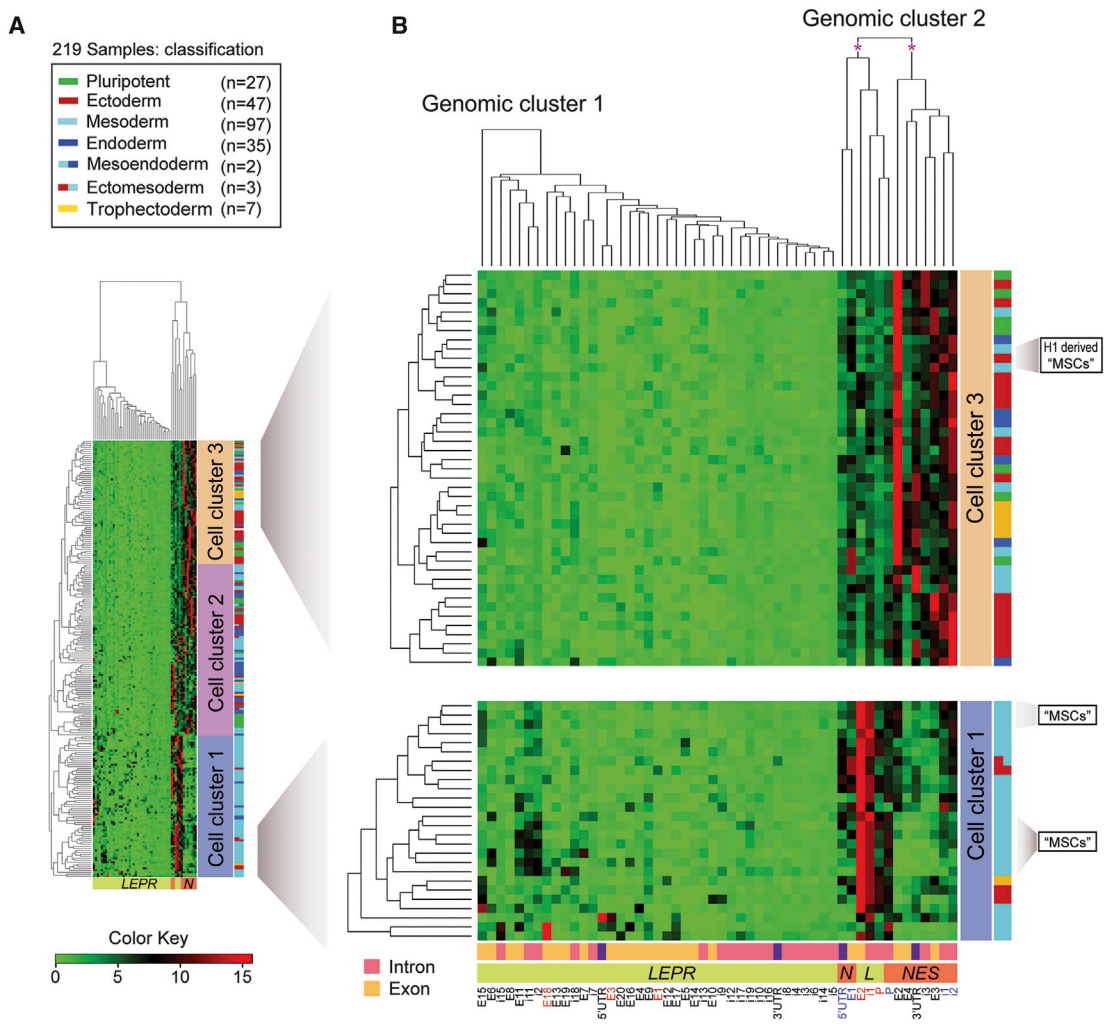

Figure 4. Representative Analysis of the Epigenetic Marker H3K4me1 at the *NES* and *LEPR* Loci

(A) Clustering analysis of deposited H3K4me1 ChiP-seq data (www.genboree.org) in 219 samples that comprise cell types from three germ layers and trophectoderm (Table S2, Figure S1). H3K4me1 data for 219 human samples (GEO accession number: GGSM621418) were imported into the Genboree Workbench from Release 9 of the Human Epigenome Atlas (www.genboree.org). Human genome assembly GRCh37/hg19 (February 2009) was used for this analysis. The normalized values for *NES* and *LEPR* were exported for cluster analysis and visualization in R (www.cran.r-project.org) using the heatmap.2 function.

(B) The enlarged views of the regions of interest are presented on the right panel. Asterisks indicate the views of truncated dendrograms. Detailed information for these dendrograms is available from Figure S1. Of note, the genomic localization of exon 20 of the *LEPR* gene is currently not available from the Human Epigenome Atlas (www.genboree.org). Hence, the epigenomic data of exon 20 should be interpreted with caution.

H1, human embryonic stem cell line H1 (WA01); H3K4me1, monomethylated histone H3 lysine 4; I, intron; *LEPR or L*, the leptin receptor gene; *LEPROT* or *Leprot*, leptin receptor overlapping transcript; "MSC," "mesenchymal stem cells"; *NES or N*, the gene coding for nestin; UTR, untranslated region.

Despite the inducible systems that enable a spatial-temporal activation of marker genes for single-cell lineage tracing, some gene-inducible systems are particularly leaky in terms of their system specificity. Moreover, the side effects of inducible reagents on a particular cell type should be taken into account. This could be exemplified by the intriguing ligand-dependent Cre recombinase that is inducible by administration of tamoxifen. Tamoxifen blocks the actions of estrogen, a female hormone, and is used to treat several types of breast cancer in clinics. It has been shown that tamoxifen has mixed estrogen-agonist effects and may alter bone and chondrocyte growth, and signal transduction between endothelial cells and pericytes (Table 1) (Chagin et al., 2007; Karimian et al.,

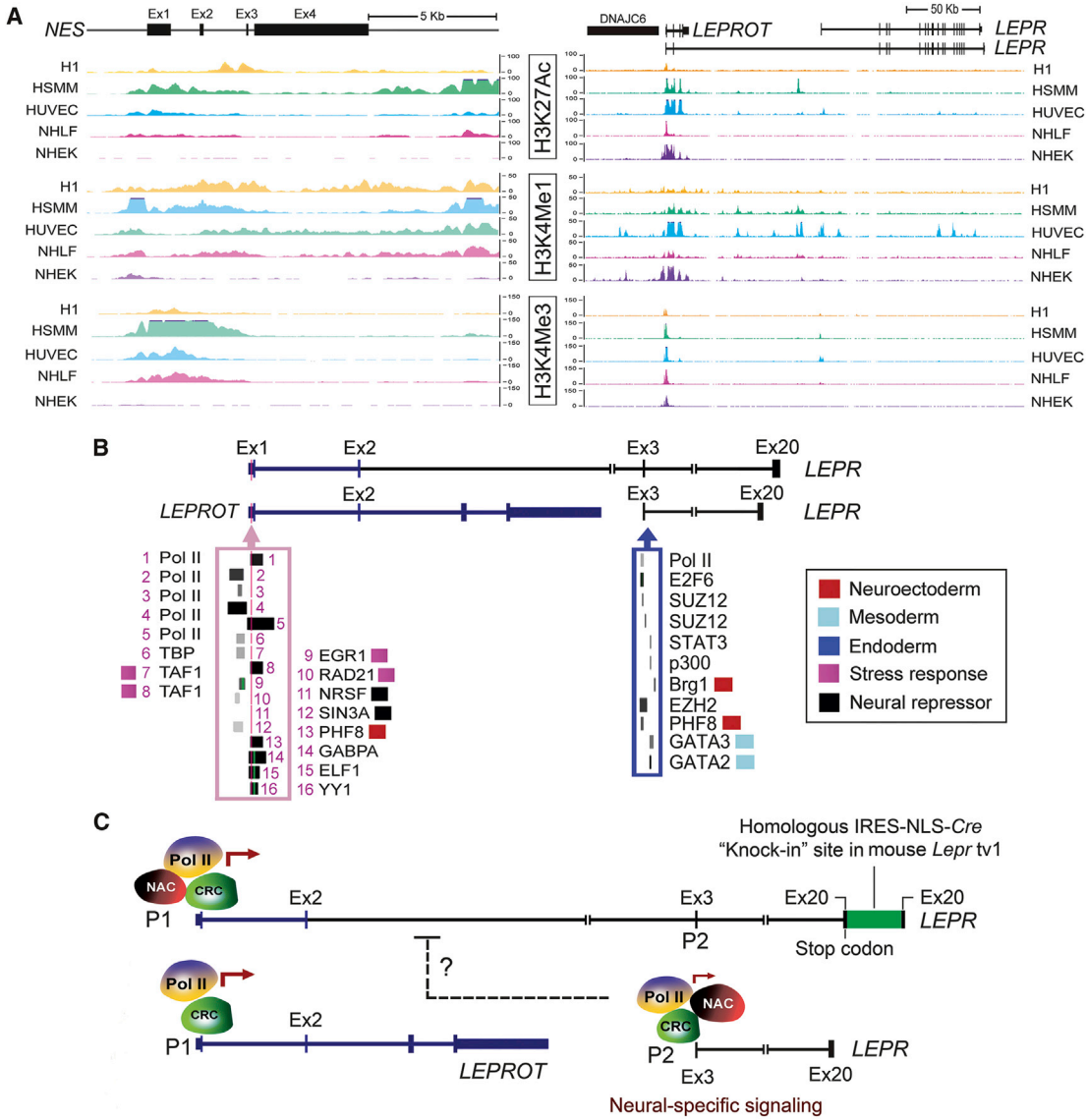

Figure 5. Deciphering Molecular Cell-Identity Codes through Integration of Data-Informatics Cascades (from Epigenomics, Transcriptomics, and Chromatin Proteomics) into Regulatory Signatures

(A) Analysis of the epigenomic markers (H3K27ac, H3K4me1, and H3K4me3 at the *NES* and *LEPR* loci) was based on the Encyclopedia of DNA Elements (ENCODE) at the UCSC (genome.ucsc.edu). Human genome assembly GRCh38/hg38 (December 2013) was used for this analysis. The ChiP-seq data are arranged to correspond precisely to their genomic locations. Five (H1, human skeletal muscle cells and myoblasts [HSMM], HUVEC, normal human lung fibroblasts [NHLF], and normal human epidermal keratinocytes [NHEK]) out of seven cell lines are shown.

(B) Mapping of transcriptional regulators on the chromatin at the *LEPR* and/or *LEPROT* loci: *LEPR* (uc001dci.4) is located at chr1:65420652-65641559, based on the orientation of the transcript variant 1 from the RefSeq NM_002303. The enriched transcriptional factors (TFs) on the *LEPR/LEPROT* gene promoter as well as the *LEPR* exon 3 regions are shown. Some of these TFs are color-highlighted based on their role in cellular response and in lineage differentiation.

(C) Multiple regulatory models for the *LEPR/LEPROT* locus: the full-length human *LEPR* gene (containing 20 exons) is transcribed from the P1 promoter. In the *Lepr*-IRES-NLS-Cre targeting construct (containing the *neo* gene, flanked by the *FRT* sites) was introduced by homologous recombination immediately after the mouse *Lepr* stop codon at exon 19 (human exon 20 counterpart) (DeFalco et al., 2001). This *Lepr*-Cre knockin mouse model has been widely used to monitor transcriptional activity of the full-length mouse *Lepr* gene that encodes the Lepr-B protein isoform (Kunisaki et al., 2013; Mizoguchi et al., 2014; Ono et al., 2014; Zhou et al., 2014).

(legend continued on next page)

2008). Furthermore, cellular cytotoxicity may be encountered in both constitutive and inducible systems. Such cytotoxicity has been observed in Cre-ER activation in induced hematological disorders (Higashi et al., 2009), thus rendering non-specific phenotypes to BM stromal cells.

It was also shown that high levels of Cre recombinase expression in mouse embryo fibroblasts induced DNA damage and inhibited cell growth in a Cre-ER activity-dependent manner (Loonstra et al., 2001), and, in neuronal stem and progenitor cells, led to increased aneuploidy, cell death, and brain developmental defects (Forni et al., 2006). These studies highlight the potential problems for developmental studies of BM cells, especially *Nes*-CreER^{T2}- and *NG2*-CreER^{TM}-expressing cells with a high neurogenic promoter or enhancer activity. Consequently, it is unknown whether there are significant amounts of *NG2*-CreER^{high} and *Nes*-CreER^{high} cells in previous studies (Acar et al., 2015; Kunisaki et al., 2013), which may be eliminated due to a high nuclear Cre activity. Hence, it is important to titrate Cre activity in each individual transgenic line, to use low levels of Cre-ER that permit for desired recombination without cell cytotoxicity, and to have tight tamoxifen-inducible controls when these Cre-based systems are used to study complicated dynamic changes of SSC and HSC niches.

Complexity of Dynamic Changes of Cellular and Molecular States in Development

Currently, the big challenge is to deeply understand the complexities of cellular and molecular states of BM cells at different developmental stages, which are thought to be tightly co-regulated by largely unknown mechanisms. At the cellular level, some cell identities present only in a transient state at a specific stage, which sometimes are too dynamic to be identified. For example, we have discussed that *Nes*-GFP^{+} and *Nes*-CreER^{T2+} cells are differentially presented in both prenatal and postnatal BMs. *Nes*-CreER^{T2} transcription may be repressed before the formation of the primary ossification center, but de-repressed after the development of the primary ossification center and the marrow cavity (Ono et al., 2014). Under the condition of tamoxifen induction at P0 and chase to P7, Isern et al. (2014) found that *Nes*-CreER^{T2+} cells were highly co-localized with *Nes*-GFP^{+} cells in BM. These data suggest that the *Nes* i2E expression is dominant at the neonatal stage (i.e., P0 to P7), which might have coupled with one core transcriptional mechanism that regulates BM stem cell niches in a developmental stage-specific manner. Of note, promoter/enhancer activity, mRNA expression, and protein expression of the marker gene of interest may be consistent or inconsistent at different developmental stages (Table S1). Thus, specific developmental windows used for induction experiments and retrieving data are required to be consistent or specifically identified for comparative studies.

Regardless of the existence of complicated cell types in BM, the underlying mechanisms that regulate their cell identities involve gene regulation not only at the transcriptional level, but also at many different molecular levels (e.g., epigenomic, post-transcriptional, and translational modifications) (Figure 3A). These complicated gene regulatory mechanisms might make transgenic data interpretation even more difficult. Therefore, we should be aware that reporter gene expression is not always consistent with its mRNA and protein expression patterns (Figure 3A). One could not assume that *Nes*-GFP^{high} cells must have high levels of endogenous *Nes* mRNAs or nestin protein expression. In general, each individual mouse strain (e.g., *Nes*-GFP or *Nes*-CreER^{T2}) should be considered as an independent assay tool for *in vivo* cell fate, functional analysis, and translational studies of mouse BM biology. In the following sections, we will further discuss the translational implication, potential challenges, and future considerations of mouse genetic models, mainly based on integrating existing genetic data and genomic informatics from both mouse and human studies (Figure 3B).

Brg1, SMARCA4 (SWI/SNF-related, matrix-associated, actin-dependent regulator of chromatin, subfamily a, member 4); CRC, chromatin-remodeling complexes including histone modifications enzymes; E2F6, E2F transcription factor 6; EGR1, early growth response 1; ELF1, E74-Like factor 1 (Ets domain transcription factor); Ex, exon; EZH2, enhancer of Zeste 2 polycomb repressive complex 2 subunit; GABPA, GA binding protein transcription factor, alpha subunit 60 kDa; GATA2, GATA binding protein 2; GATA3, GATA binding protein 3; H1, H1 (WA01) human embryonic stem cell line; HSMM, human skeletal muscle myoblasts (mesoderm); HUVEC, human umbilical vein endothelial cells (mesoderm) from blood vessels; *LEPROT*, leptin receptor overlapping transcript; NAC: neuronal lineage activator complexes that include either BRG1 or PHF8 or both; NHEK, normal human epidermal keratinocytes (ectoderm); NHLF, normal human lung fibroblasts; NRSF, known as REST (RE1-silencing transcription factor); P1, the promoter of the canonical *LEPR* gene; P2, an alternative promoter at the 5′ of exon 3 of *LEPR*; p300, EP300 (E1A binding protein P300); PHF8, PHD finger protein 8, a histone lysine demethylase that preferentially acts on histones in the monomethyl or dimethyl states; Pol II, RNA polymerase II; RAD21, RAD21 cohesin complex component; SIN3A, SIN3 transcription regulator family member A; STAT3, signal transducer and activator of transcription 3 (acute-phase response factor); SUZ12, SUZ12 polycomb repressive complex 2 subunit; TAF1, TAF1 RNA polymerase II, TATA-box binding protein (TBP)-associated factor, 250 kDa; TBP, TATA-box binding protein; YY1, YY1 transcription factor.

Mouse Genetic Models versus Human Resource Databases: Translational Relevance, Challenges, and Prospective Considerations

In the biomedical field, the ultimate goals of using diverse animal models are to provide translatable biomedical information to understand the etiology of human diseases and to derive effective clinical treatments for patients. On the one hand, the success of this translational approach relies on the understanding of the interplay of datasets between murine models and the human cells. On the other hand, the availability of genome-wide datasets in the post human genome era offers the possibility to optimize mouse genetic models through existing coherent human datasets (Birney et al., 2007; Kundaje et al., 2015) (Figure 3B). However, the above interplay approaches have not been well integrated to guide stem cell research. Here, we will focus on the interpretation of mouse model data based on the transcriptomic complexity of marker gene transcripts in both humans and mice. Furthermore, we will shed light on how "generic" epigenomic markers from redundant human epigenomic databases could provide prospective molecular cell identities for facilitating translational biology.

Transcriptomic Complexity of Marker Gene Transcripts

To better integrate human genomic data with mouse models, we initially analyzed the genomic organization of the human *NES* and *LEPR* loci, due to the availability of datasets, and because the two reporters, *Nes*-GFP and *Lepr*-Cre, have been extensively used to categorize stem cell identities in animal models as discussed above (Tables 1 and S1). Figure 1A illustrates the genomic organization of these two genes from mice, rats, and humans. In the case of the homolog genes that encode the nestin protein, there are significantly conserved intronic and exonic structures, but with some variations found in the 20- to 25-kb 5′ genomic regions (Figure 1A). Likely, the similar genomic organizations of *Nes* and *NES* among mice, rats, and humans would make *in vivo* animal studies more relevant to clinical sittings.

However, with respect to the leptin receptor genes, genomic sequence data reveal significant differences between the species in terms of gene structures, function, transcription start sites, alternative transcripts, and the locations of the last exon in each individual transcript (Figure 1B). During embryonic development, *LEPR* isoform *A* (*LEPR-A*) is expressed in fetal liver, hematopoietic tissues, and the choroid plexus. In adults, *LEPR-A* is highly expressed in mesoendoderm-derived tissues (such as heart, liver, small intestine, prostate, and ovary) (www.SWISS_Prot). However, *LEPR-B* (the canonical isoform) is highly expressed in neuroectodermal tissues, including the choroid plexus and hypothalamus, in adult humans and mice (Figure 1B). Notably, in humans, there are at least five LEPR protein isoforms derived from six mRNA transcripts, which are expressed in a tissue-specific manner (Figure 1B). Thus, this genomic or proteomic information is particularly useful for us to design GFP- or Cre-based *Lepr* constructs in murine models to study tissue-specific regulation of cellular states.

Furthermore, the *LEPR* and *LEPROT* (leptin receptor overlapping transcripts) genes, which encode two distinct proteins, share the same promoter and the first two exons (Figure 1B). The orientation of the two genes are similar in both human and rat genomes, but different from that of mice (Figure 1B). The mouse *Leprot* is approximately 50 kb away from *Lepr* (Figure 1B). Importantly, we need to determine where the reporter activity is initiated. The differential activation of *LEPR* and *LEPROT* promoters or enhancers may render opposite interpretations of the results.

Generic Epigenomic Markers and Molecular Cell Identities

Redundant epigenomic databases represent a valuable tool for defining various epigenomic and transcriptional states during development. It is unknown whether we could also accurately define molecular cell identities using a panel of "generic" epigenomic markers, which are currently available in miscellaneous human epigenomic databases. We evaluated the presence or absence of the monomethylated histone H3 lysine four epigenomic marker (H3K4me1), at the human *NES* and *LEPR* loci, enabled by the availability of a large H3K4me1 chromatin immunoprecipitation sequencing (ChiP-seq) dataset in 219 human cell samples (www.genboree.org). The 219 samples comprise cell types from all three germ layers and the trophectoderm (Table S2; Figure S1). H3K4me1 usually pre-marks the enhancers that are not active, but primed for activation, in the absence of external stimuli or signals (Shlyueva et al., 2014). As shown in Figure 4, the dendrogram reveals two genomic clusters that separate the majority of marked introns and exons of *LEPR* from those of *NES* (Figures 4A and 4B). Moreover, H3K4me1 segregates the previously well-characterized regulatory regions (i.e., intron 1 and 2 enhancers, denoted as i1E and i2E, respectively) of the *NES* (or *Nes*) gene, validating the reliability of using H3K4me1 for cell-identity classification in this analysis. Therefore, H3K4me1 segregates all samples into three major cell clusters, in which cell clusters 1 and 3 are clearly different (Figures 4A and 4B). Cell cluster 1 (containing predominantly mesodermal derivatives) is apparently regulated by H3K4me1 on the promoter region, intron 1, and exon 2 of the *LEPR* gene (Figure 4B, lower panel). Interestingly, H3K4me1 marks cell cluster 3, containing predominantly neural and epidermal/ectodermal derivatives (e.g., brain and foreskin tissues), on introns 1 and 2 of the *NES* promoter (Figure 4B, upper panel). The inclusion of pluripotent stem cells and their differentiated cell types in the cell cluster 3 merely reflects the developmental

proximity between the neuroectoderm and embryonic epiblasts. Cell cluster 2, which partially overlaps with the cell clusters 1 and 3, requires additional markers to identify their cell identities. Nevertheless, these data suggest that even a generic marker (such as H3K4me1) on limited genomic loci (e.g., *LEPR* and *NES*) could bear remarkable epigenetic information to classify mesodermal and ectodermal disparities.

Accordingly, we further analyzed three major epigenomic markers, H3K27ac, H3K4me1, and H3K4me3, at the *NES* and *LEPR* loci, based on the Encyclopedia of DNA Elements at UCSC (2003–2012) (genome.ucsc.edu). Unlike H3K4me1, H3K27ac marks active enhancers at transcriptional factor-accessible genomic loci (Creyghton et al., 2010), whereas H3K4me3 marks gene promoters that are active or poised to be active (Benayoun et al., 2014; Lauberth et al., 2013). In brief, we were able to integrate data-informatics cascades from epigenomics, transcriptomics, and chromatin proteomics into regulatory complexes for monitoring cell identity in human embryonic stem cell line H1 (WA01) and other mesodermal or ectodermal cell lines (i.e., human skeletal muscle cells and myoblasts, HUVECs [human umbilical vein endothelial cells], normal human lung fibroblasts, and normal human epidermal keratinocytes) (Figure 5A). Mapping of potential transcriptional regulators on chromatin at the *NES* and *LEPR* loci (e.g., at BM stromal cell cluster 1, Figure 4B) would provide new insights into *Nes*-GFP and *Lepr*-Cre transcriptome activities that are commonly monitored in mouse models.

Indeed, *LEPR* represents a complicated regulation due to the presence of multiple alternative transcripts and the co-regulated *LEPROT* gene (Figure 1B). The three histone markers are increased on the promoter region adjacent to exons 1 and 2 among the four cell lines (except H1) (Figure 5A, right panel). Interestingly, H3K4me1 was located at multiple regions in intron 2 and in two 3′ exonic areas in HUVECs (Figure 5A, right panel). The biological consequences of these sites remain unclear. However, they might be associated with alternative transcription start sites of the gene, therefore potentially interfering with *Lepr*-Cre transcriptome interpretation in endothelial cells. Based on the recruitment of RNA polymerase II, we identified at least two promoters (i.e., P1 and P2) on the full-length *LEPR*. The two promoters appear to be consistent with their epigenetic states (Figures 5A, right panel, 5B, and 5C). These data confirm the presence of alternative transcripts due to differential initiation of transcription under diverse cellular contexts.

Interestingly, a neuronal repressor complex (that involves both NRSF and SIN3A) was drastically downregulated at the P1 promoter. Concomitantly, there is an increase in neural activation complex (NAC) that contains PFH8, GABPA, and ELF1 at the both P1 and P2 promoters (Figures 5B and 5C). The P2 promoter (located at the 5′ end of exon 3) seems to be a weaker promoter compared with P1. Moreover, P2 is apparently regulated by the NAC that includes either BRG1 or PHF8 (or both), polycomb group repressive complex proteins (e.g., EZH2 and SUZ12), and GATA binding proteins (e.g., GATA2 and GATA3) (Figure 5B). Thus, a neural-specific regulation of the P2 promoter has been implicated in the human *LEPR* gene (Satoh et al., 2009).

Taken together, transcription factor profiling of the *LEPR* promoters reveals a potential molecular switch between neuroectodermal and mesodermal regulation, suggesting a possible coupling mechanism between sequential derepression and activation, which controls cell-type-specific transcriptional activity at the P1 and P2 promoters (Figure 5C). Of note, we need to be aware of using eipgenomic data from human cell lines, which might increase the possibility of altered epigenetic marker expression under certain cell culture conditions. In the future, these analyses should include large-scale epigenomic data from human tissues and purified human cell populations. It would be also desirable to have a side-by-side comparative analysis between mouse and human epigenomic datasets. Ultimately, we would be able to make humanized mouse models by integrating partial human genomic or epigenomic information into a transgenic mouse model for translational studies.

Concluding Remarks

Constitutive and inducible expression based on various types of transgenes have identified a plethora of functionally important stem cell and progenitor populations in BM. Various experimental discrepancies, data irreproducibility, and misinterpretations could be explained, minimized, and circumvented if we have a better understanding of these mouse genetic systems. Ideally, we should develop and apply non-toxic, cell-type-specific, regulatable, and humanized mouse genetic systems, combined with other technological approaches for *in vivo* cell-fate analysis. Theoretically, molecular signatures of cell identities could be evident at multiple levels of gene regulation, resulting in activation of transcriptional complexes, mRNA transcription, and protein translation at different developmental stages. Practically, we need to be aware of these differences when we interpret data based on mouse reporter activity (e.g., from *Nes*-GFP, *Nes*-CreER, and *Lepr*-Cre), mRNA transcripts, and protein expression. Each gene regulation or expression mechanism should be considered as an independent assay for lineage analysis. Importantly, all genetic and epigenetic assays should be combined with definitive surface marker analysis and genome-wide "clusterome" to accurately define specific

cellular states and cell identities. Precise understanding of the regulation of reporter transcriptomes in murine models would enable us to accurately decipher diverse cell fates in the BM.

SUPPLEMENTAL INFORMATION

Supplemental Information includes one figure and two tables and can be found with this article online at https://doi.org/10.1016/j.stemcr.2017.09.014.

ACKNOWLEDGMENTS

This work was supported by the Intramural Research Program of the NIH at the National Institute of Neurological Disorders and Stroke (to K.G.C. and K.R.J.) and the National Institute of Dental and Craniofacial Research (to P.G.R.). We thank Dr. Ronald D. McKay for discussion and support of this work.

REFERENCES

Acar, M., Kocherlakota, K.S., Murphy, M.M., Peyer, J.G., Oguro, H., Inra, C.N., Jaiyeola, C., Zhao, Z., Luby-Phelps, K., and Morrison, S.J. (2015). Deep imaging of bone marrow shows non-dividing stem cells are mainly perisinusoidal. Nature *526*, 126–130.

Ara, T., Tokoyoda, K., Sugiyama, T., Egawa, T., Kawabata, K., and Nagasawa, T. (2003). Long-term hematopoietic stem cells require stromal cell-derived factor-1 for colonizing bone marrow during ontogeny. Immunity *19*, 257–267.

Asada, N., Kunisaki, Y., Pierce, H., Wang, Z., Fernandez, N.F., Birbrair, A., Ma'ayan, A., and Frenette, P.S. (2017). Differential cytokine contributions of perivascular haematopoietic stem cell niches. Nat. Cell Biol. *19*, 214–223.

Balordi, F., and Fishell, G. (2007). Mosaic removal of hedgehog signaling in the adult SVZ reveals that the residual wild-type stem cells have a limited capacity for self-renewal. J. Neurosci. *27*, 14248–14259.

Benayoun, B.A., Pollina, E.A., Ucar, D., Mahmoudi, S., Karra, K., Wong, E.D., Devarajan, K., Daugherty, A.C., Kundaje, A.B., Mancini, E., et al. (2014). H3K4me3 breadth is linked to cell identity and transcriptional consistency. Cell *158*, 673–688.

Bianco, P., and Robey, P.G. (2015). Skeletal stem cells. Development *142*, 1023–1027.

Bianco, P., Cao, X., Frenette, P.S., Mao, J.J., Robey, P.G., Simmons, P.J., and Wang, C.Y. (2013). The meaning, the sense and the significance: translating the science of mesenchymal stem cells into medicine. Nat. Med. *19*, 35–42.

Birney, E., Stamatoyannopoulos, J.A., Dutta, A., Guigo, R., Gingeras, T.R., Margulies, E.H., Weng, Z., Snyder, M., Dermitzakis, E.T., Thurman, R.E., et al. (2007). Identification and analysis of functional elements in 1% of the human genome by the ENCODE pilot project. Nature *447*, 799–816.

Buch, T., Heppner, F.L., Tertilt, C., Heinen, T.J., Kremer, M., Wunderlich, F.T., Jung, S., and Waisman, A. (2005). A Cre-inducible diphtheria toxin receptor mediates cell lineage ablation after toxin administration. Nat. Methods *2*, 419–426.

Chagin, A.S., Karimian, E., Zaman, F., Takigawa, M., Chrysis, D., and Savendahl, L. (2007). Tamoxifen induces permanent growth arrest through selective induction of apoptosis in growth plate chondrocytes in cultured rat metatarsal bones. Bone *40*, 1415–1424.

Cohen, P., Zhao, C., Cai, X., Montez, J.M., Rohani, S.C., Feinstein, P., Mombaerts, P., and Friedman, J.M. (2001). Selective deletion of leptin receptor in neurons leads to obesity. J. Clin. Invest. *108*, 1113–1121.

Creyghton, M.P., Cheng, A.W., Welstead, G.G., Kooistra, T., Carey, B.W., Steine, E.J., Hanna, J., Lodato, M.A., Frampton, G.M., Sharp, P.A., et al. (2010). Histone H3K27ac separates active from poised enhancers and predicts developmental state. Proc. Natl. Acad. Sci. USA *107*, 21931–21936.

Danielian, P.S., White, R., Hoare, S.A., Fawell, S.E., and Parker, M.G. (1993). Identification of residues in the estrogen receptor that confer differential sensitivity to estrogen and hydroxytamoxifen. Mol. Endocrinol. *7*, 232–240.

Danielian, P.S., Muccino, D., Rowitch, D.H., Michael, S.K., and McMahon, A.P. (1998). Modification of gene activity in mouse embryos in utero by a tamoxifen-inducible form of Cre recombinase. Curr. Biol. *8*, 1323–1326.

DeFalco, J., Tomishima, M., Liu, H., Zhao, C., Cai, X., Marth, J.D., Enquist, L., and Friedman, J.M. (2001). Virus-assisted mapping of neural inputs to a feeding center in the hypothalamus. Science *291*, 2608–2613.

Ding, L., and Morrison, S.J. (2013). Haematopoietic stem cells and early lymphoid progenitors occupy distinct bone marrow niches. Nature *495*, 231–235.

Feil, R., Wagner, J., Metzger, D., and Chambon, P. (1997). Regulation of Cre recombinase activity by mutated estrogen receptor ligand-binding domains. Biochem. Biophys. Res. Commun. *237*, 752–757.

Feltri, M.L., D'Antonio, M., Previtali, S., Fasolini, M., Messing, A., and Wrabetz, L. (1999). P0-Cre transgenic mice for inactivation of adhesion molecules in Schwann cells. Ann. N. Y. Acad. Sci. *883*, 116–123.

Forni, P.E., Scuoppo, C., Imayoshi, I., Taulli, R., Dastru, W., Sala, V., Betz, U.A., Muzzi, P., Martinuzzi, D., Vercelli, A.E., et al. (2006). High levels of Cre expression in neuronal progenitors cause defects in brain development leading to microencephaly and hydrocephaly. J. Neurosci. *26*, 9593–9602.

Frenette, P.S., Pinho, S., Lucas, D., and Scheiermann, C. (2013). Mesenchymal stem cell: keystone of the hematopoietic stem cell niche and a stepping-stone for regenerative medicine. Annu. Rev. Immunol. *31*, 285–316.

Friedenstein, A.J., Piatetzky, S., II, and Petrakova, K.V. (1966). Osteogenesis in transplants of bone marrow cells. J. Embryol. Exp. Morphol. *16*, 381–390.

Higashi, A.Y., Ikawa, T., Muramatsu, M., Economides, A.N., Niwa, A., Okuda, T., Murphy, A.J., Rojas, J., Heike, T., Nakahata, T., et al. (2009). Direct hematological toxicity and illegitimate chromosomal recombination caused by the systemic activation of CreERT2. J. Immunol. *182*, 5633–5640.

Isern, J., Garcia-Garcia, A., Martin, A.M., Arranz, L., Martin-Perez, D., Torroja, C., Sanchez-Cabo, F., and Mendez-Ferrer, S. (2014). The neural crest is a source of mesenchymal stem cells with specialized hematopoietic stem cell niche function. Elife *3*, e03696.

Kalajzic, I., Kalajzic, Z., Kaliterna, M., Gronowicz, G., Clark, S.H., Lichtler, A.C., and Rowe, D. (2002). Use of type I collagen green fluorescent protein transgenes to identify subpopulations of cells at different stages of the osteoblast lineage. J. Bone Miner. Res. *17*, 15–25.

Karimian, E., Chagin, A.S., Gjerde, J., Heino, T., Lien, E.A., Ohlsson, C., and Savendahl, L. (2008). Tamoxifen impairs both longitudinal and cortical bone growth in young male rats. J. Bone Miner. Res. *23*, 1267–1277.

Kfoury, Y., and Scadden, D.T. (2015). Mesenchymal cell contributions to the stem cell niche. Cell Stem Cell *16*, 239–253.

Kuhn, R., Schwenk, F., Aguet, M., and Rajewsky, K. (1995). Inducible gene targeting in mice. Science *269*, 1427–1429.

Kundaje, A., Meuleman, W., Ernst, J., Bilenky, M., Yen, A., Heravi-Moussavi, A., Kheradpour, P., Zhang, Z., Wang, J., et al.; Roadmap Epigenomics Consortium (2015). Integrative analysis of 111 reference human epigenomes. Nature *518*, 317–330.

Kunisaki, Y., Bruns, I., Scheiermann, C., Ahmed, J., Pinho, S., Zhang, D., Mizoguchi, T., Wei, Q., Lucas, D., Ito, K., et al. (2013). Arteriolar niches maintain haematopoietic stem cell quiescence. Nature *502*, 637–643.

Lagace, D.C., Whitman, M.C., Noonan, M.A., Ables, J.L., DeCarolis, N.A., Arguello, A.A., Donovan, M.H., Fischer, S.J., Farnbauch, L.A., Beech, R.D., et al. (2007). Dynamic contribution of nestin-expressing stem cells to adult neurogenesis. J. Neurosci. *27*, 12623–12629.

Lauberth, S.M., Nakayama, T., Wu, X., Ferris, A.L., Tang, Z., Hughes, S.H., and Roeder, R.G. (2013). H3K4me3 interactions with TAF3 regulate preinitiation complex assembly and selective gene activation. Cell *152*, 1021–1036.

Lendahl, U., Zimmerman, L.B., and McKay, R.D. (1990). CNS stem cells express a new class of intermediate filament protein. Cell *60*, 585–595.

Lewis, A.E., Vasudevan, H.N., O'Neill, A.K., Soriano, P., and Bush, J.O. (2013). The widely used Wnt1-Cre transgene causes developmental phenotypes by ectopic activation of Wnt signaling. Dev. Biol. *379*, 229–234.

Littlewood, T.D., Hancock, D.C., Danielian, P.S., Parker, M.G., and Evan, G.I. (1995). A modified oestrogen receptor ligand-binding domain as an improved switch for the regulation of heterologous proteins. Nucleic Acids Res. *23*, 1686–1690.

Logan, M., Martin, J.F., Nagy, A., Lobe, C., Olson, E.N., and Tabin, C.J. (2002). Expression of Cre recombinase in the developing mouse limb bud driven by a Prxl enhancer. Genesis *33*, 77–80.

Loonstra, A., Vooijs, M., Beverloo, H.B., Allak, B.A., van Drunen, E., Kanaar, R., Berns, A., and Jonkers, J. (2001). Growth inhibition and DNA damage induced by Cre recombinase in mammalian cells. Proc. Natl. Acad. Sci. USA *98*, 9209–9214.

Mendez-Ferrer, S., Scadden, D.T., and Sanchez-Aguilera, A. (2015). Bone marrow stem cells: current and emerging concepts. Ann. N. Y. Acad. Sci. *1335*, 32–44.

Mignone, J.L., Kukekov, V., Chiang, A.S., Steindler, D., and Enikolopov, G. (2004). Neural stem and progenitor cells in nestin-GFP transgenic mice. J. Comp. Neurol. *469*, 311–324.

Mizoguchi, T., Pinho, S., Ahmed, J., Kunisaki, Y., Hanoun, M., Mendelson, A., Ono, N., Kronenberg, H.M., and Frenette, P.S. (2014). Osterix marks distinct waves of primitive and definitive stromal progenitors during bone marrow development. Dev. Cell *29*, 340–349.

Morikawa, S., Mabuchi, Y., Niibe, K., Suzuki, S., Nagoshi, N., Sunabori, T., Shimmura, S., Nagai, Y., Nakagawa, T., Okano, H., et al. (2009). Development of mesenchymal stem cells partially originate from the neural crest. Biochem. Biophys. Res. Commun. *379*, 1114–1119.

Morrison, S.J. (2014). Time to do something about reproducibility. Elife *3*. https://doi.org/10.7554/eLife.03981.

Morrison, S.J., and Scadden, D.T. (2014). The bone marrow niche for haematopoietic stem cells. Nature *505*, 327–334.

Oguro, H., Ding, L., and Morrison, S.J. (2013). SLAM family markers resolve functionally distinct subpopulations of hematopoietic stem cells and multipotent progenitors. Cell Stem Cell *13*, 102–116.

Ono, N., Ono, W., Mizoguchi, T., Nagasawa, T., Frenette, P.S., and Kronenberg, H.M. (2014). Vasculature-associated cells expressing nestin in developing bones encompass early cells in the osteoblast and endothelial lineage. Dev. Cell *29*, 330–339.

Owen, M., and Friedenstein, A.J. (1988). Stromal stem cells: marrow-derived osteogenic precursors. Ciba Found. Symp. *136*, 42–60.

Sacchetti, B., Funari, A., Remoli, C., Giannicola, G., Kogler, G., Liedtke, S., Cossu, G., Serafini, M., Sampaolesi, M., Tagliafico, E., et al. (2016). No identical "mesenchymal stem cells" at different times and sites: human committed progenitors of distinct origin and differentiation potential are incorporated as adventitial cells in microvessels. Stem Cell Reports *6*, 897–913.

Satoh, T., Yoshino, S., Katano, A., Ishizuka, T., Tomaru, T., Shibusawa, N., Hashimoto, K., Yamada, M., and Mori, M. (2009). Isolation of a novel leptin receptor gene promoter preferentially functioning in neuronal cells. Biochem. Biophys. Res. Commun. *389*, 673–677.

Shlyueva, D., Stampfel, G., and Stark, A. (2014). Transcriptional enhancers: from properties to genome-wide predictions. Nat. Rev. Genet. *15*, 272–286.

Sugiyama, T., Kohara, H., Noda, M., and Nagasawa, T. (2006). Maintenance of the hematopoietic stem cell pool by CXCL12-CXCR4 chemokine signaling in bone marrow stromal cell niches. Immunity *25*, 977–988.

Sun, M.Y., Yetman, M.J., Lee, T.C., Chen, Y., and Jankowsky, J.L. (2014). Specificity and efficiency of reporter expression in adult neural progenitors vary substantially among nestin-CreER(T2) lines. J. Comp. Neurol. *522*, 1191–1208.

Tronche, F., Kellendonk, C., Kretz, O., Gass, P., Anlag, K., Orban, P.C., Bock, R., Klein, R., and Schutz, G. (1999). Disruption of the glucocorticoid receptor gene in the nervous system results in reduced anxiety. Nat. Genet. *23*, 99–103.

Yamauchi, Y., Abe, K., Mantani, A., Hitoshi, Y., Suzuki, M., Osuzu, F., Kuratani, S., and Yamamura, K. (1999). A novel transgenic technique that allows specific marking of the neural crest cell lineage in mice. Dev. Biol. *212*, 191–203.

Zhou, B.O., Yue, R., Murphy, M.M., Peyer, J.G., and Morrison, S.J. (2014). Leptin-receptor-expressing mesenchymal stromal cells represent the main source of bone formed by adult bone marrow. Cell Stem Cell *15*, 154–168.

Zhu, X., Bergles, D.E., and Nishiyama, A. (2008). NG2 cells generate both oligodendrocytes and gray matter astrocytes. Development *135*, 145–157.

Zhu, X., Hill, R.A., Dietrich, D., Komitova, M., Suzuki, R., and Nishiyama, A. (2011). Age-dependent fate and lineage restriction of single NG2 cells. Development *138*, 745–753.

Zimmerman, L., Parr, B., Lendahl, U., Cunningham, M., McKay, R., Gavin, B., Mann, J., Vassileva, G., and McMahon, A. (1994). Independent regulatory elements in the nestin gene direct transgene expression to neural stem cells or muscle precursors. Neuron *12*, 11–24.

Stem Cell Reports, Volume *9*

Supplemental Information

Mouse Genetic Analysis of Bone Marrow Stem Cell Niches: Technological Pitfalls, Challenges, and Translational Considerations

Kevin G. Chen, Kory R. Johnson, and Pamela G. Robey

Table S1. Developmental Stage-Related Marker Gene Expression in Bone Marrow Stem Cell Lineages: Conditions and Constrains in Murine Models

Stages	Mouse strains/cells	Major findings & descriptions	CFU-F	Authors' comments	References
E8.5-, E10.5-, E18.5	*Nes*-CreER^{T2}: RCE-loxP	Tamoxifen induction at E8.5 & E10.5, chase to E18.5: *Nes*-Cre^{+} cells, not found in proliferating and hypertrophic chondrocytes, infiltrate over osteochondral junction and into the trabecular bone.	0.8%	BM *Nes*-Cre^{+} cells do not contribute to fetal endochondrogenesis.	(Isern et al., 2014)
E9.5	*Sox10*-CreER^{T2}	Among 18% of Sox10-Cre^{+} cells, 72% of them were *Nes*-GFP^{+}/PDGFRα^{+} cells.	NA	Evidence of *Nes*-GFP^{+} cells' neural crest association	(Isern et al., 2014)
E10.5	*Nes*-GFP^{+}/ CD31^{+} cells	Represent 8% of endothelial cells at limb buds	NA	Appeared at the endochrondral condensation stage	(Ono et al., 2014)
E11.5	*Nes*-GFP^{+}/ CD31^{+} cells	Observed at the perichondrium	NA	*Nes*-GFP^{+} cells are rarely found within the mesenchymal condensation region.	(Ono et al., 2014)
E11.5-P0, P21	*Nes*-CreER^{T2}: Rosa26 tomato	Tamoxifen induction (from E11.5) before the formation the POC and chase to P0 and P21: only few *Nes*-Cre^{+} cells found in bone at P0 and P21	NA	After the POC, *Nes*-Cre^{+} cells do not commit to neonatal and postnatal bone development.	(Ono et al., 2014)
E12.5	*Nes*-GFP^{+} /CD31^{-} cells	1st appearance at the perichondrium	NA	None	(Ono et al., 2014)
E13.5	*Nes*-GFP^{+} /CD31$^{+/-}$ cells	►Overlap with Col2^{+} cells at the perichondrium ►Some *Nes*-GFP^{+} cells are likely derived from collagen II-expressing (chondrogenic) cells. ►Perichondral *Nes*-GFP^{+}CD31$^{+/-}$ cells are regulated by both Ihh and Runx2.	NA	*Nes*-GFP^{+}/CD31^{-} non-endothelial cells become osteoprogenitor cells upon Ihh and Runx2 induction.	(Ono et al., 2014)
E13.5	*Nes*-CreER^{T2}: RCE-loxP	Similar to *Nes*-GFP^{+} cells: detected near the chondral–perichondral interface and the osteo-chondral junction	NA	Consistent with the dynamic nature of *Nes*-GFP^{+} cells	(Isern et al., 2014)
E13.5-P0, P21	*Nes*-CreER^{T2}: Rosa26 tomato	Tamoxifen induction and chase from E13.5: only few *Nes*-Cre^{+} cells found in bone at P0 and P21	NA	After the POC, *Nes*-Cre^{+} cells do not commit to neonatal and postnatal bone development.	(Ono et al., 2014)
E14.5	*Nes*-GFP^{+} /CD31$^{+/-}$cells	Both types of *Nes*+ cells occupied at the inner perichondrium, with *Nes*-GFP^{+} /CD31^{-} cells aligned on the innermost portion.	NA	None	(Ono et al., 2014)
E15.5	*Nes*-GFP^{+} /CD31$^{+/-}$ cells	►Infiltrate into the cartilage template along vascular invasion ►Increase in *Nes*-GFP^{+}/CD31$^{+/-}$ cell numbers ►*Nes*-GFP^{+}CD31$^{+/-}$ closely associated at the POC	NA	*Nes*-GFP^{+}/CD31^{+} cells show (at least 3-fold) stronger GFP signals than *Nes*-GFP^{+}/CD31^{-} cells at E15.5, suggesting that *Nes*-GFP transcription is positively regulated by endothelial cell signaling.	(Ono et al., 2014)
E15.5	*Lepr*-Cre	Absence of *Lepr*-Cre^{+} cells at the POC at this stage		*Nes*-GFP^{+} and *Osx*-Cre^{+} emerged in the POC	(Mizoguchi et al., 2014)
E15.5	*Nes*-creER^{T2}: iDTR mice	Deletion of *Nes*-Cre^{+} cells in this double transgenic mice resulted in 4-fold decrease in HSC activity in fetal BM within 48 hours, concomitantly with 8-fold increase in HSCs in fetal liver	NA	These data suggest that *Nes*-GFP transcriptome positively regulates the migration of HSC niches from the embryonic liver to the BM.	(Isern et al., 2014)
E16.5-P7, P21	*Nes*-CreER^{T2}: *Rosa26 tomato*	Tamoxifen induction at E16.5, the time that the marrow space starts to form, and chase to P7 and P21: see larger numbers of *Nes*-Cre^{+} in bone	0.3%,	*Nes*-CreER transcription is repressed before the formation of POC, but derepressed after the formation of the POC and marrow cavity.	(Ono et al., 2014)
E17.5	*Lepr*-Cre^{+} cells	►1st appearance of *Lepr*-Cre^{+} cells ►Found in the primary spongiosa and the periosteum	NA	*Lepr*-Cre^{+} cells in the periosteum might be originated from *Nes*-GFP^{+}/CD31$^{+/-}$ cells as described by Ono et al. 2014.	(Mizoguchi et al., 2014)
E17.5	*Nes*-GFP^{+} cells	Display 3-fold lower CFU-Fs than *Nes*-GFP^{-} cells, but higher capacity to form "mesenspheres"	0.1%	Higher SCC potential in *Nes*-GFP^{+} cells than *Nes*-GFP^{-} cells	(Isern et al., 2014)

E17.5	*Nes*-GFP$^+$ cells	Not associated with *Col2.3*-Cre$^+$ cells and chondrocytes	0.1%	Distinction from osteoblastic cells	(Isern et al., 2014)
E18.5	*Nes*-GFP$^+$ cells	Frequently associated with arterioles and nascent CD31$^+$ endothelial cells within the osteochondral junction; but not with osterix (by antibody staining);	0.8%	►Express endogenous *Nes* mRNAs at this stage ►CFU-F frequency 6-fold lower than *Nes*-GFP$^-$ cells	(Isern et al., 2014)
E18.5-P1, Peri-natal	*Nes*-GFP$^+$ cells	►*Nes*-GFP$^+$ cells, likely derived from neural crest ►Secrete the HSC niche factor Cxcl12 ►Distinguished from mesoderm derived "MSCs" ►Do not generate fetal chondrocytes	0.2%	►Perinatal stages: from E18.5 to postnatal day 1 (www.jax.org) ► "MSCs" are an incorrect terminology that depicts BM SSCs.	(Isern et al., 2014)
E19.5	*Lepr*-Cre: dTomato; Col2.3-GFP	*Lepr*-Cre$^+$ cells were rare and had no contribution to bone development at this stage.	NA	Used for explicitly identifying osteoblastic bone-lining cells	(Zhou et al., 2014)
P0	*Nes*-GFP$^+$ cells	Belong to BM CD45$^-$/CD31$^-$/Ter119$^-$ stromal cells	0.2%	P0, neonatal stage	(Isern et al., 2014)
P0	*Nes*-GFP$^+$ /PDGFRα^- cells	►*Nes*-GFP$^+$ cells are close to HSCs (within 20 µm) in the neonatal BM. ►Express mRNAs (e.g., *Sox10*, *Plp1*, *Erbb3*, and *Dhh*), typically presented in Schwann cell precursors ►No *Gfap* found in mature Schwann cells	0.2%	►Give rise to distinct HSC niche-forming stromal cells *in vivo* ►Have a high glial differentiation propensity *in vitro*	(Isern et al., 2014)
P0	*Nes*-GFP$^+$ /PDGFRα^+ cells	►Enriched mRNA transcripts associated with HSC niche maintenance genes (e.g. *Cxcl12*, *KitL*, *Angpt1*, and *Lepr*), may have a role in HSC maintenance ►Have an *in vitro* mesodermal (adipocyte) differentiation propensity	0.2%	►*Nes*-GFP$^+$ cells show physical proximity to the HSC niche. ►Osteoblastic differentiation genes were selectively inhibited during enforced HSC mobilization or Adrb3 activation (Mendez-Ferrer et al. 2010).	(Isern et al., 2014)
P0.5	*Lepr*-Cre: dTomato: *Col2.3*-GFP	►A drastic increase in the number of *Lepr*-Cre$^+$ cells in metaphysis ►The emergence of few *Lepr*-Cre$^+$/Col2.3-GFP$^+$ osteoblasts in trabecular bone	NA	This probably is the earliest osteogenic contribution made by *Lepr*-Cre$^+$ cells, highlighting the 1st plausible postnatal SSC niche at the metaphyseal and trabecular regions.	(Zhou et al., 2014)
P0-P7	*Nes*-CreER^{T2}	Tamoxifen induction at P0 and chase to P7: highly colocalized with BM *Nes*-GFP$^+$ cells	0.3%	Two transcriptional mechanisms for *Nes*-GFP are consistent at this stage, suggesting the two reporter systems might share an enhancer complex at the intron 2 of the *Nes* gene.	(Isern et al., 2014)
P0-P14	*Nes*-GFP: *Nes*-CreER^{T2}	Tamoxifen induction at the neonatal stage (P0): *Nes-GFP*$^+$ cells overlap with *Nes*-CreER^{T2+} cells.	0.3%	It appears that *Nes*-Cre$^+$ cells partially overlay with *Nes-GFP*$^+$ cells at BM blood vessels, but not in *Nes*-GFP$^+$ perivascular pericytes.	(Isern et al., 2014)
P3	*Nes*-GFP$^+$ cells	CFU-F activity much lower than *Nes*-GFP$^-$ cells	0.3%	None	(Isern et al., 2014)
P3	*Nes*-GFP: *Tie2*-Cre	94% *Nes*-GFP$^+$/*Tie2*-Cre$^+$/CD45$^-$ cells	NA	*Nes*-GFP$^+$ cells have a role in specifying endothelial cells.	(Ono et al., 2014)
P3-P5	*Nes*-GFP: *Nes*-CreER^{T2}	Tamoxifen induction at P3 and chase to P5: ►Almost 100% *Nes*-GFP$^+$/*Nes*-Cre$^+$ cells ►81% *Nes*-Cre$^+$/CD31$^+$ cells at the primary spongiosa and BM ►34% *Nes*-GFP$^+$/CD31$^+$ endothelial cells ►*Nes*-GFP$^+$/*Nes*-CreER$^+$ cells also express endogeneous *Nes* mRNAs and the nestin protein (detected by flow cytometry using ab6142). ►*Nes* mRNA (by quantitative PCR) increased by 82-, 263-, and 414-fold in *Nes*-GFP$^+$/*Nes*-Cre$^-$CD31$^-$, *Nes*-GFP$^+$/*Nes*-Cre$^-$CD31$^+$, and *Nes*-	NA	►*Nes*-Cre is inducible at 48 hours after tamoxifen administration ►Both *Nes*-GFP$^+$ and *Nes*-Cre$^+$ cells likely share a transcriptional mechanism at this stage. ►*Nes*-Cre transcriptional activity is dominant over *Nes*-GFP in CD31$^+$ endothelial cells. ►Additional transcriptional activators from endothelial cells are needed to drive endogenous *Nes* mRNA expression to a high level.	(Ono et al., 2014)

		GFP$^+$/*Nes*-Cre$^+$, respectively, relative to *Nes*-GFP negative control			
P3-P5, P10, P17, P24, 4w	*Nes*-creER^{T2}: Rosa26 tomato: Col1(2.3kb)-GFP	Tamoxifen induction at P3 and chase up to 1 month (4 weeks or 4w): ►10% *Nes*-Cre$^+$ osteoblasts expressing Col1 at P5 ►*Nes*-Cre$^+$ cells increased up to 26% and 23% at P10 and P17 respectively ►*Nes*-Cre$^+$ decreased to 5% and 3% at P24 and 4w respectively	NA	*Nes*-Cre$^+$ cells have limited contribution to osteoblasts at the postnatal stage (within one month).	(Ono et al., 2014)
P3-P10	*Nes*-GFP: *Osx*-CreER	Tamoxifen induction at P3 and chase to P10: 96% of cells targeted by *Osx*-CreER were positive for *Nes*-GFP (i.e. *Nes*-GFP$^+$/*Osx*-CreER$^+$).	NA	*Nes*-GFP$^+$ cells might have a major role in specifying osteoblasts at this stage.	(Ono et al., 2014)
P3-P10	*Nes*-GFP: *Col1*(3.2kb)-CreER	Tamoxifen induction at P3 and chase to P10: 92% *Nes*-GFP$^+$/*Col1*(3.2kb)-CreER$^+$	NA	The same comment as above	(Ono et al., 2014)
P3-P10	*Nes*-GFP: *Ocn*-CreER	Tamoxifen induction at P3 and chase to P10: 93% *Nes*-GFP$^+$/*Ocn*-Cre$^+$	NA	The same comment as above	(Ono et al., 2014)
P3-24w	*Nes*-CreER^{T2}: Rosa26 tomato	Tamoxifen induction at P3 and chase 6 months (24 weeks or 24w): ►*Nes*-Cre$^+$ cells distributed from the BM to the growth plate; 84% *Nes*-CreER$^+$ /CD31$^+$ cells; ►*Nes*-Cre$^+$ descendant cells form reticular sinusoidal endothelial cells for at least 24 weeks. ►*Nes*-Cre$^+$ cells generate few osteoblasts, osteocytes, and chondrocytes; but no adipocytes	NA	In adult BM, *Nes*-Cre$^+$ cells mainly contribute to sinusoidal endothelial cells.	(Ono et al., 2014)
P5-P6	*Nes*-GFP: iOsx/Tomato	Tamoxifen induction at P5 and chase to P6: ~38% of iOsx$^+$ cells were *Nes*-GFP$^+$ in bone tissues.	NA	P5-iOsx$^+$ BM cells exhibit a trilineage differentiation potential.	(Mizoguchi et al., 2014)
P5-4w	iOsx/Tomato	Tamoxifen induction at P5: increased CFU-F frequency of sorted iOsx/Tomato$^+$ cells in the BM stroma harvested at 4 weeks after tamoxifen injection	0.5% at 4w	None	(Mizoguchi et al., 2014)
P5-15w	*Nes*-GFP: iOsx/Tomato;	Tamoxifen induction at P5 and chase to 15w in CD45$^-$/Ter119$^-$/CD31$^-$/iOsx$^+$ BM stromal cells: 78% *Nes*-GFP$^+$/Lepr$^+$ (using anti-Lepr), in which 89% of cells were PDGFRα^+ and 83% of cells PDGFRβ^+	NA	►Regulation of *Nes*-GFP and *Lepr* is converged at this stage, apparently for the maturation of bone development. ►No Western blots used to define the size of the Lepr protein in this and other studies.	(Mizoguchi et al., 2014)
P5-15w, 16w, 19w	*Lepr*-Cre: *Osx*-Cre /Tomato	*Osx*-Cre/Tomato mice pulsed at P5 and fracture wound started in 15w-old *Lepr*-Cre/Tomato mice: ►Observed freshly made chondrogenic zones of the fracture callus at day 8 (total 16w) ►No *Osx*-Cre$^+$ chondrocytes observed after 3w chase (total 19w)	NA	See comments to P5-32w below.	(Mizoguchi et al., 2014)
P5-32w-33w	*Lepr*-Cre: *Osx*-Cre /Tomato	Osx-Cre/Tomato mice pulsed at P5 and fracture wound started in 32w-old mice: ►Some *Lepr*-Cre$^+$ cells, identified as Sox9$^+$ cells in the fractured callus, contributed to progenitors of osteocytes, chondrocytes, and adipocytes *in vivo*. ►*Lepr*-Cre+ cells not colocalized well with the Lepr protein in the non-fracture callus region ►No Lepr protein detected (by an antibody from R&D Systems) in the fracture callus at day 8 (33w)	NA	These data suggest the Lepr protein is not required for the skeletal repair, thus reinforcing the role of *Lepr* transcriptomes as pivotal indicators of skeletal development.	(Mizoguchi et al., 2014)
P7	*Nes*-GFP$^+$	~2.4-fold decrease in *Nes* mRNAs relative	0.3%	Evidence of a dynamic *Nes*	(Isern et al.,

	cells	to E18.5		transcriptome	2014)
P7	*Lepr*-Cre$^+$ cells	►Distributed throughout the BM cavity ►~92% *Lepr*-Cre$^+$ cells also positive for *Nes*-GFP in the BM ►Positive for *Nes*-GFP and *Osx*-Cre in the primary spongiosa	NA	The emergence of *Lepr*-Cre dominance (in the developing bone and BM) coincides with the decrease of *Nes*-GFP transcriptional activity, suggesting a coordinate regulation between the *Lepr* and *Nes* genes.	(Mizoguchi et al., 2014)
P7	Gfap$^+$ cells	Schwann cells expressing Gfap detected in the BM	0.3%	Gfap: a marker for non-myelin-forming Schwann cells	(Isern et al., 2014)
P7	*Nes*-GFP: *Wnt1*-Cre2	Increase in *Wnt1*-Cre2-traced osteochondral cells; partially overlap with *Nes*-GFP$^+$ cells, including perivascular *Nes*-GFP$^+$ cells	0.3%	Wnt1 is not a specific marker for neural crest cells.	(Isern et al., 2014)
P7	*Nes*-GFP	►*Nes*-GFP$^+$ cells distributed at the diaphysis and metaphysis (close to the growth plate) in endochondral bones ►*Nes*-GFP^{high} cells traced perivascular cells in the primary spongiosa and pericytes of the arterioles in diaphysis ►*Nes*-GFP^{low} cells in osteoblasts on the bone surface, osteocytes, and endothelial cells	NA	See comments on *Nes*-GFP expression at 8w described by Ono et al., 2014	(Ono et al., 2014)
P7	*Nes*-GFP: *Lepr*-Cre	97% *Nes*-GFP$^+$/*Lepr*-Cre$^+$/CD45$^-$ cells	NA	*Nes*-GFP$^+$ cells may have a role in specifying *Lepr*-Cre$^+$ SSCs.	(Ono et al., 2014)
P7	*Nes*-GFP: Osx-Cre	98% *Nes*-GFP$^+$/*Osx*-Cre$^+$/CD45$^-$ cells	NA	*Nes*-GFP$^+$ cells are associated with osteoblast development.	(Ono et al., 2014)
P7 & more stages	*Mx1-Cre*	►*Mx1*-Cre labels non-hematopoietic and non-endothelial osteogenic cells in the bone. ►*Mx1-Cre*$^+$ cells are highly enriched at the postnatal day 7. ►*Mx1-Cre*$^+$ cells are resided at the perivascular niche and enriched in the CD105$^+$/CD140a$^+$ subset (43%) and calvarial sutures. ►59% *Nes*-GFP$^+$ cells overlap with *Mx-1*$^+$ cells. ►*Mx1*-Cre$^+$ stromal cells are lineage-restricted, essential for supplying new osteoblasts, and for fracture healing *in vivo*. ► *Mx1*-Cre$^+$ cells are clonogenic, having tripotent differentiation potential *in vitro* and *in vivo*. ► *Mx1*-Cre labels mature osteogenic cells that express osterix, osteopontin, and osteocalcin.	High	►*Nes*-GFP$^+$ cells may be the precursor of *Mx1*-cre$^+$ cells. ►*Mx1*-Cre$^+$ cells may contribute to pre-osteoblasts. ►No chondrogenesis is required for adult bone fracture repair. ►*Mx1*-Cre-labeled cells partially overlap with nestin$^+$ cells detected by an anti-nestin antibody (Millipore, clone rat-401). ►*Mx1*-Cre can be used to distinguish long-term osteogenic cells from other bone-forming cells. ►The osteoblastic turnover rates vary at different developmental stages.	(Park et al., 2012)
P14	*Nes*-GFP$^-$ cells	More than 100-fold decrease in CFU-F activity in *Nes*-GFP$^-$ BM stromal cells compared with E18.5 cells	~0%	Unknown mechanisms to regulate this critical transition	(Isern et al., 2014)
P21	*Nes*-GFP$^+$ cells	Maintain steady CFU-F activity	0.3%	None	(Isern et al., 2014)
P21	*Lepr*-Cre$^+$ cells	Distributed throughout the BM cavity, but not on the endosteum	NA	See comments on *Lepr*-Cre$^+$ cells at 15w	(Mizoguchi et al., 2014)
P28	*Wnt1*-Cre2$^+$ cells	CFU-F activity was much higher in *Wnt1*-Cre2$^+$ cells than in *Wnt1*-Cre2$^-$ BM stromal cells.	0.2%	See above comments.	(Isern et al., 2014)
5w	*Nes*-GFP	*Nes*-GFP$^+$ cells clustered, but not colocolized, with osterix$^+$ cells (by immunostaining) in trabecular bone sections	NA	None	(Mendez-Ferrer et al., 2010)
7w-12w	*Nes*-GFP^{high} cells	►Exceptionally low, 0.002% of BM cells ►Quiescent, only along arterioles ►NG2$^+$ and α-smooth muscle actin$^+$	High	►Likely have an HSC-niche-supporting role ►Neither *Nes*-GFP^{high} nor *Nes*-	(Kunisaki et al., 2013)

		pericytes ►Physically associated with tyrosine hydroxylase (HT) positive sympathetic nerves and GFAP$^+$ Schwann cells ►Do not overlap with *Lepr*-Cre$^+$ cells		GFP^{low} BM stromal cells seem to express endogenous *Nes* mRNAs by microarray (Mendez-Ferrer et al., 2010) and by RNA sequencing (Kunisaki et al., 2013).	
7w-12w	*Nes*-GFP^{low} cells	Abundant, reticular in shape, mainly associated with perisinusoids and overlap with *Lepr*-Cre$^+$ cells	Low	Likely pericytes for SSCs	(Kunisaki et al., 2013)
7w-12w	*Nes*-GFP^{high} /*Lepr*-Cre$^-$ cells	►*Nes*-GFP^{high}/*Lepr-cre*$^-$ cells express the highest level of *Scf* and *Cxcl12*. ►RNA-seq data showed that *Nes*-GFP^{high}/*Lepr-cre*$^-$ cells were negative for *Nes* and positive for *Lepr* expression (GSE48764).	NA	►Discrepancy between transcriptome and transcriptional activity ►Evidence of a putative inverse regulation between the *Nes* and *Lepr* genes	(Kunisaki et al., 2013)
7w-12w	*Nes*-GFP: *NG2*-CreER	*Nes*-GFP^{high} cells (~30%), not *Nes*-GFP^{low} cells, colocalized with *NG2*-Cre$^+$ cells	NA	None	(Kunisaki et al., 2013)
7w-12w	*NG2*-CreER: iDTR	►Tamoxifen induction and diphtheria toxin treatment depleted ~55% of *Nes*-GFP^{high} cells. ►Depletion of NG2$^+$ cells expelled quiescent HSCs from arteriolar to perisinusoidal niches.	NA	*NG2*-Cre$^+$ cells are believed to be part of HSC niches, which endorses HSC for quiescence.	(Kunisaki et al., 2013)
8w	*Nes*-GFP	In endochondral bones: ►*Nes*-GFP^{high} cells were decreased in the primary spongiosa and BM. ►*Nes*-GFP^{low} cells were further decreased in osteoblasts (on bone surfaces), osteocytes, but still observable at this stage.	NA	From P7 to 8w, *Nes*-GFP$^{high/low}$ cells continue to decrease without a conclusive mechanism.	(Ono et al., 2014)
8w	*Lepr*-Cre$^+$ /*Col2.3*-GFP$^-$	*Lepr*-Cre$^+$/*Col2.3*-GFP$^-$/CD45$^-$/Ter119$^-$ /CD31$^-$ BM cells ►Cell frequency stabilized near 0.2% ►Quiescent at 8w, reactivable under stress conditions ►Intrafemoral injection of 500 of these cells generated adipocytes, osteocytes, and chondrocytes at 4w.	NA	These data suggest that *Lepr*-Cre$^+$/*Col2*.3-GFP$^-$ cells are a progenitor cell source for adipocytes and osteolineage cells.	(Zhou et al., 2014)
8w	*Nes*-CreER^{T2}: *Scf*$^{fl/-}$	Deletion of Scf from *Nes*-Cre$^+$cells did not affect HSC frequency in BM.	NA	HSC niche maintenance does not require SCF from *Nes*-Cre$^+$ cells.	(Ding and Morrison, 2013)
8w	*Nes-GFP*	*Nes*-GFP^{high} along larger vessels in BM; *Nes*-GFP^{low} in perisinusoidal stromal cells similar to *Scf*-GFP$^+$ cells	NA	*Nes*-GFP expression patterns in this study are consistent with the report by Mendez-Ferrer et al. 2010.	(Ding and Morrison, 2013)
8w	*Nes-Cre*$^+$ *cells*	Only found around larger blood vessels in BM	NA	*Nes* expression discrepancies	(Ding and Morrison, 2013)
8w	*Nes-Cherry: Nes-GFP*	*Nes-Cherry*$^+$ cells were around larger vessels but not around sinusoids, whereas *Nes*-GFP$^+$ cells were detected around both regions.	NA	*Nes*-Cherry has a similar expression pattern to that of *Nes*-Cre. However, the detail information about *Nes*-Cherry mice is not available.	(Ding and Morrison, 2013)
8w (2m)	*Lepr*-Cre: dTomato: *Col2.3*-GFP	*Lepr*-Cre$^+$ cells were filled with metaphysis and diaphysis of the BM,	NA	The emergence of 3-10% *Lepr*-Cre$^+$/*Col2.3*-GFP$^+$ osteoblasts in bone	(Zhou et al., 2014)
8w-16w	*Wnt1*-CreER	*Wnt1*-CreER$^+$/CD45$^-$/Ter119$^-$ BM stromal cells	0.5%	*Wnt1*-Cre$^+$ neural crest derivatives minimally contribute to CFU-F colonies at this stage.	(Zhou et al., 2014)
8w-12w	*Nes*-GFP: Lepr	70% of Lepr$^+$ cells (by flow cytometric analysis) in BM mainly overlap with *Nes*-GFP$^+$ cells.	NA	None	(Pinho et al., 2013)
8w-12w	PDGFRα^+ /CD51$^+$	PDGFRα^+/CD51$^+$ cells represent a small subset of *Nes*-GFP$^+$ cells. *Nes* mRNAs are expressed in this cell population.	NA	Expression of CD51 (the integrin subunit αV) enhances *Nes* mRNA expression and might enable to convert *Nes*-GFP$^+$/PDGFRα^+	(Pinho et al., 2013)

				/CD146$^+$ cells into perivascular pericytes.	
8w-12w	α-catulin-GFP$^+$ cells	►Represent 0.02% of BM hematopoietic cells, located at the central perisinusoids ►Restricted to HSC niche cells, adjacent to *Lepr*$^+$ and Cxcl12$^+$ cells, ►Distant from arterioles and endosteal surface ►HSCs located within the 10 μm sinusoidal vessels with an HSC frequency of 1/6	NA	These data are inconsistent with periarteriolar HSC-niches supported by *NG2*–CreER$^+$ cells in a previous report (Kunisaki et al. 2013).	(Acar et al., 2015)
8w-12w	Gfap$^+$ cells	Gfap$^+$ non-myelinating Schwann cells associated with nerve fibers tend to localize in the central BM.	NA	Indirect evidence of an HSC-niche supporting role by neural crest lineage cells	(Acar et al., 2015)
8w-12w	*NG2*-CreER$^+$ cells	►Not detected in *Scf*-GFP$^+$ or Cxcl12-DsRed$^+$ cells ►*NG2*-CreER mediated conditional deletion of Scf in Scf$^{GFP/fl}$ mice or Cxcl12 in *NG2*–CreER: Cxcl12$^{-/fl}$ mice did not affect HSC frequency.	NA	*Nes*-Cre mediated deletion of *Scf* also shows no effects on HSC function (Ding et al. 2012).	(Acar et al., 2015)
8w-12w	HSCs	Higher HSC density, marked by α-catulin-GFP$^+$/c-kit$^+$, found in the diaphysis than in metaphysis	NA	An unexpected result that might provide insights into HSC niche dynamics	(Acar et al., 2015)
8w-16w	BM stromal cells	CD45$^-$/Ter119$^-$ non-hematopoietic BM cells	1.4%	None	(Zhou et al., 2014)
8w-16w	PDFFRα+	PDGFRα$^+$/CD45$^-$/Ter119$^-$ BM stromal cells	10%	None	(Zhou et al., 2014)
8w-16w	PDFFRα$^+$ /Sca-I$^+$	The PDGFRα$^+$/Sca-1$^+$/CD45$^-$/Ter119$^-$ cell population	16%	Reside mainly around arterioles, but does not express the HSC niche factor Cxcl12	(Zhou et al., 2014)
8w-16w	PDFFRα$^+$ /Sca-1$^-$	The PDGFRα$^+$/Sca-1$^-$/CD45$^-$/Ter119$^-$ cell population, known as CXCL12-abundant reticular (CAR) cells	8%	Exist primarily around sinusoids and express high levels of Cxcl12	(Zhou et al., 2014)
8w-16w	*Lepr*-Cre /Tomato$^+$ /CD105$^+$	►0.3% *Lepr*-Cre$^+$/CD45$^-$/Ter119$^-$ cells ►98% PDFFRα$^+$, 98% CD51$^+$, 69% CD105$^+$ ►Around sinusoids and arterioles ►High levels of *Lepr* mRNAs ►The Lepr protein detected by immunostaining ►Considered as a major source of BM SSCs	14%	►Tripotent cells from 9% of CFU-F colonies ►Ossicles from 30% CFC-F colonies ►CD105, known as endoglin, a plasma membrane and extracellular glycoprotein of vascular endothelial cells, used as an “MSC” marker	(Zhou et al., 2014)
8w-16w	*Lepr*-Cre /Tomato$^-$ CD105$^-$	*Lepr*-Cre/Tomato$^-$/CD105$^-$/CD45$^-$/Ter119$^-$ BM stromal cells	1%	14-fold decrease in CFU-F colonies compared with *Lepr*-Cre/Tomato$^+$ /CD105$^+$ cells	(Zhou et al., 2014)
8w-16w	*Lepr*-Cre /Tomato$^+$	*Lepr*-Cre/Tomato$^+$/CD45$^-$/Ter119$^-$ BM stromal cells	11%	Around sinusoids and arterioles	(Zhou et al., 2014)
8w-16w	*Lepr*-Cre/Tomato$^-$	*Lepr*-Cre/Tomato$^-$/CD45$^-$/Ter119$^-$ BM stromal cells	0.1%	Depletion of CFU-F capacity	(Zhou et al., 2014)
8w-16w	*Lepr-Cre*$^+$ /Scf-GFP$^+$	*Lepr*-Cre/Tomato$^+$/*Scf*-GFP$^+$/CD45$^-$ /Ter119$^-$ BM stromal cells	NA	Around sinusoids only	(Zhou et al., 2014)
8w-16w	*Prx1*-Cre /Tomato$^+$	*Prx1*-Cre/Tomato$^+$/CD45$^-$/Ter119$^-$ BM stromal cells	10%	A positive marker for BM stromal cells, tightly associated with *Lepr*-Cre	(Zhou et al., 2014)
8w-16w	*Scf*-GFP$^+$	*Scf*-GFP$^+$/CD45$^-$/Ter119$^-$ BM stromal cells	10%	A positive marker for BM stromal cells	(Zhou et al., 2014)
8w-16w	Cxcl12-DsRed^{high}	Cxcl12-DsRed^{high}/CD45$^-$/Ter119$^-$ BM stromal cells	12%	A positive marker for BM stromal cells	(Zhou et al., 2014)
8w-16w	*Nes*-GFP^{low}	*Nes*-GFP^{low}/CD45$^-$/Ter119$^-$ BM stromal cells	8%	A positive marker for BM stromal cells	(Zhou et al., 2014)
8w-16w	*Nes*-GFP^{high}	*Nes*-GFP^{high}/CD45$^-$/Ter119$^-$ BM stromal cells	3%	See comments on *NG2*-CreER$^+$ cells	(Zhou et al., 2014)
8w-16w	*Nes*-CreER$^+$	*Nes*-CreER$^+$/CD45$^-$/Ter119$^-$ BM stromal cells	0	A negative marker for BM stromal cells	(Zhou et al., 2014)

8w-16w	*NG2*-CreER^{+}	*NG2*-CreER^{+}/CD45^{-}/Ter119^{-} BM stromal cells	2%	*NG2*-Cre^{+} and *Nes*-GFP^{+} cells show similar low CFU-F activity.	(Zhou et al., 2014)
8w-16w	*Mx1*-CreER^{+}	*Mx1*-CreER^{+}/CD45^{-}/Ter119^{-} BM stromal cells	2%	*Mx1*-Cre seems a weaker marker for osteoblastic lineage at this stage.	(Zhou et al., 2014)
12w-16w	*Prx1*-Cre; Jak2^{V617F}	►Jak2 mutant cells had a 3-fold decrease in CFU-F activity compared with the wild-type cells. ►Increase in adipocytes	Low	Genetic evidence indicates Jak2/Stat3 is underlying the regulation of both adipogenesis and osteogenesis.	(Yue et al., 2016)
12w-16w	*Nes*-creER^{T2}: RCE-loxP	Pulsed with tamoxifen at 3 months and chased for 4w (1 month): No *Nes*-Cre^{+} osteoblasts, osteocytes, and chondrocytes (collagen α1 type 2^{+})	NA	*Nes*-Cre mediates slow turnover of osteolineage cells.	(Mendez-Ferrer et al., 2010)
12w-44w	*Nes*-creER^{T2}: RCE-loxP	Pulsed with tamoxifen at 3 months (12w) and chased for 8 months (44w): see GFP^{+} osteoblasts, osteocytes, and chondrocytes (collagen α1 type 2^{+})	NA	Adult *Nes*-Cre^{+} cells are likely an SSC source.	(Mendez-Ferrer et al., 2010)
15w	*Lepr*-Cre^{+} cells	Distributed not only in the BM cavity, but also along the cortical bone as *Lepr*-/Cre^{+}/Ocn^{+}/DMP1^{+} osteoblasts and osteocytes	NA	This study suggests a migration route of *Lepr*-Cre^{+} cells during osteogenesis: BM cavity → endosteum → trabecular bone → cortical bone.	(Mizoguchi et al., 2014)
24w	*Prx1*-Cre /*Lepr*$^{fl/fl}$	Conditional deletion of *Lepr* in SSCs: increased osteogenesis and down-regulated adipogenesis	NA	The Lepr protein is likely an inhibitor of adult osteogenesis.	(Yue et al., 2016)
24w, 40w, 56w	*Lepr*-Cre: dTomato: *Col2.3*-GFP	Age-dependent contribution of *Lepr*-Cre^{+} cells to bone development: 24w: 10%–23% of *Col2.3*-GFP^{+} cells, 40w: 43%–67% of *Col2.3*-GFP^{+} cells, 56w: 61%–81% of *Col2.3*-GFP^{+} cells	NA	Accordingly, no Lepr protein expression was detected by IF (at 10m or 40w), which suggests that *Lepr*-Cre functions as an independent transcriptional reporter in these stages	(Zhou et al., 2014)

ABBREVIATIONS:

Adrb3, β3 adrenoreceptor; BM, bone marrow; CFU-F, Colony forming unit-fibroblastic, an assay based on freshly isolated single cells from an intact tissue, in which single cells are able to initiate clonal growth of fibroblastic cells at low density; Col1, collagen I; DMP1, dentin matrix protein 1; HSC, hematopoietic stem cell; iDTA, diphtheria toxin; iDTAR, diphtheria toxin receptor; IF, immunofluorescence; m, month(s); MSC, “mesenchymal stem cells”; NA, not available; *Nes*-CreER^{T2}, tamoxifen-inducible transgenic mouse described by Balordi and Fishell (2007); Ocn, osteocalcin; Osx, osterix; POC, primary ossification center; SSC, skeletal stem cell; Tripotent: osteochondrogenic, osteogenic, and adipogenic; wk, week

REREFERNCES

Acar, M., Kocherlakota, K.S., Murphy, M.M., Peyer, J.G., Oguro, H., Inra, C.N., Jaiyeola, C., Zhao, Z., Luby-Phelps, K., and Morrison, S.J. (2015). Deep imaging of bone marrow shows non-dividing stem cells are mainly perisinusoidal. Nature 526, 126-130.

Balordi, F., and Fishell, G. (2007). Mosaic removal of hedgehog signaling in the adult SVZ reveals that the residual wild-type stem cells have a limited capacity for self-renewal. J Neurosci 27, 14248-59.

Ding, L., and Morrison, S.J. (2013). Haematopoietic stem cells and early lymphoid progenitors occupy distinct bone marrow niches. Nature 495, 231-235.

Isern, J., García-García, A., Martín, A.M., Arranz, L., Martín-Pérez, D., Torroja, C., Sánchez-Cabo, F., Méndez-Ferrer, S. (2014). The neural crest is a source of mesenchymal stem cells with specialized hematopoietic stem cell niche function. Elife 25; 3:e03696.

Kunisaki, Y., Bruns, I., Scheiermann, C., Ahmed, J., Pinho, S., Zhang, D., Mizoguchi, T., Wei, Q., Lucas, D., Ito, K., et al. (2013). Arteriolar niches maintain haematopoietic stem cell quiescence. Nature 502, 637-643.

Mendez-Ferrer, S., Michurina, T.V., Ferraro, F., Mazloom, A.R., Macarthur, B.D., Lira, S.A., Scadden, D.T., Ma'ayan, A., Enikolopov, G.N., and Frenette, P.S. (2010). Mesenchymal and haematopoietic stem cells form a unique bone marrow niche. Nature 466, 829-834.

Mizoguchi, T., Pinho, S., Ahmed, J., Kunisaki, Y., Hanoun, M., Mendelson, A., Ono, N., Kronenberg, H.M., and Frenette, P.S. (2014). Osterix marks distinct waves of primitive and definitive stromal progenitors during bone marrow development. Dev Cell 29, 340-349.

Ono, N., Ono, W., Mizoguchi, T., Nagasawa, T., Frenette, P.S., and Kronenberg, H.M. (2014). Vasculature-associated cells expressing nestin in developing bones encompass early cells in the osteoblast and endothelial lineage. Dev Cell 29, 330-339.

Park, D., Spencer, J.A., Koh, B.I., Kobayashi, T., Fujisaki, J., Clemens, T.L., Lin, C.P., Kronenberg, H.M., and Scadden, D.T. (2012). Endogenous bone marrow MSCs are dynamic, fate-restricted participants in bone maintenance and regeneration. Cell Stem Cell 10, 259-72.

Pinho, S., Lacombe, J., Hanoun, M., Mizoguchi, T., Bruns, I., Kunisaki, Y., and Frenette, P.S. (2013). PDGFRalpha and CD51 mark human nestin+ sphere-forming mesenchymal stem cells capable of hematopoietic progenitor cell expansion. J Exp Med 210, 1351-1367.

Yue, R., Zhou, B.O., Shimada, I.S., Zhao, Z., and Morrison, S.J. (2016). Leptin Receptor Promotes Adipogenesis and Reduces Osteogenesis by Regulating Mesenchymal Stromal Cells in Adult Bone Marrow. Cell Stem Cell 18, 782-796.

Zhou, B.O., Yue, R., Murphy, M.M., Peyer, J.G., and Morrison, S.J. (2014). Leptin-receptor-expressing mesenchymal stromal cells represent the main source of bone formed by adult bone marrow. Cell Stem Cell 15, 154-168.

Figure S1

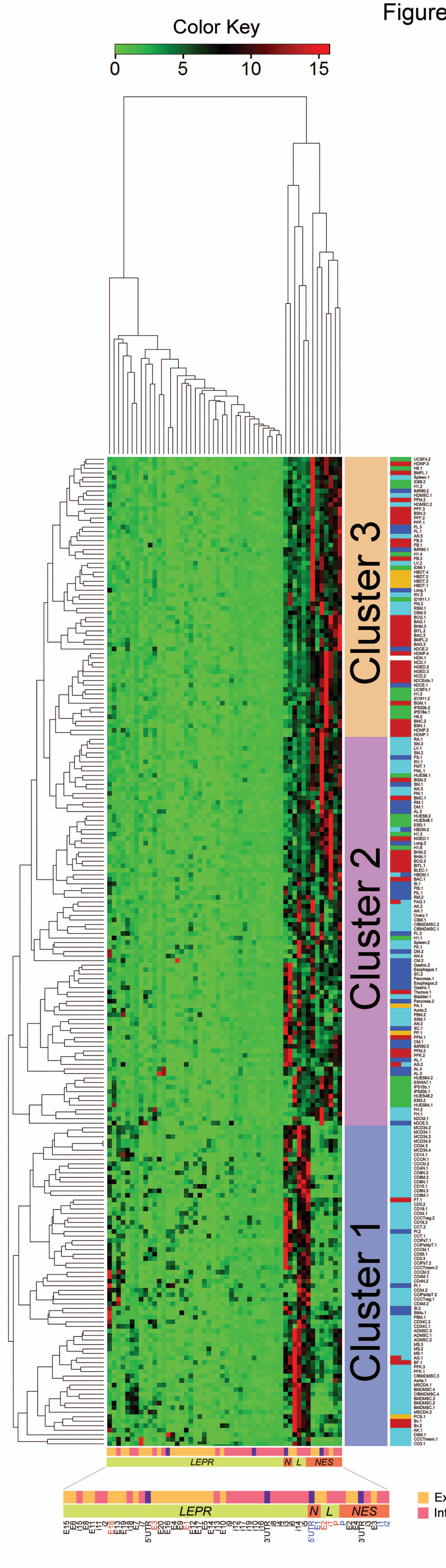
Color Key
0
5
10
15
Cluster 3
Cluster 2
Cluster 1
LEPR
N
L
NES
5'UTR
3'UTR
Exon
Intron